© 2018. Published by The Company of Biologists Ltd | Development (2018) 145, dev162651. doi:10.1242/dev.162651

RESEARCH ARTICLE

PDGF-A suppresses contact inhibition during directional collective cell migration

Martina Nagel and Rudolf Winklbauer*

ABSTRACT

The leading-edge mesendoderm (LEM) of the *Xenopus* gastrula moves as an aggregate by collective migration. However, LEM cells on fibronectin *in vitro* show contact inhibition of locomotion by quickly retracting lamellipodia upon mutual contact. We found that a fibronectin-integrin-syndecan module acts between p21-activated kinase 1 upstream and ephrin B1 downstream to promote the contact-induced collapse of lamellipodia. To function in this module, fibronectin has to be present as puncta on the surface of LEM cells. To overcome contact inhibition in LEM cell aggregates, PDGF-A deposited in the endogenous substratum of LEM migration blocks the fibronectin-integrin-syndecan module at the integrin level. This stabilizes lamellipodia preferentially in the direction of normal LEM movement and supports cell orientation and the directional migration of the coherent LEM cell mass.

KEY WORDS: Collective migration, Contact inhibition, Fibronectin, Integrin, Ephrin B1, PDGF-A

INTRODUCTION

Individually migrating cells often show contact inhibition of locomotion. When they collide, their forward movement ceases and the cells reorient and move apart. This process typically includes the collapse of locomotory protrusions upon cell-cell contact (Abercrombie and Dunn, 1975; Stramer and Mayor, 2016). Contact repulsion between individually translocating cells *in vivo* can regulate cell dispersal (Bard and Hay, 1975; Villar-Cerviño et al., 2013; Davis et al., 2015). During collective migration, loose streams, such as those formed by *Xenopus* neural crest cells, can use contact inhibition to orient cell motile behavior. Where cells are in contact, protrusions are inhibited, but when free space is available, for example at the leading edge of the cell mass, cells extend processes, and this orients the overall movement of the stream (Carmona-Fontaine et al., 2008).

Contact inhibition of protrusive activity is less understood when cells migrate as a coherent sheet. Despite their tight adhesion to neighbors, cells can extend 'cryptic' lamellipodia on the substratum, which contribute to the translocation of the cell mass (e.g. Farooqui and Fenteany, 2005; Vasilyev et al., 2009; Gutzeit, 1991; Lewellyn et al., 2013; Hayer et al., 2016). Moreover, cells can use the surface of adjacent cells as substratum for migration. For example, border cell clusters in the *Drosophila* ovary require cadherin-mediated adhesion to nurse cells for translocation (Niewiadomska et al., 1999). This could be explained by a basic absence of contact inhibition in the respective cells, as in malignant cells (Abercrombie, 1979) or in premigratory neural crest cells (Scarpa et al., 2015). Positive regulation of protrusive activity, for example by chemotactic factors, would then be sufficient to endow collectively migrating cells with locomotory processes. Alternatively, contact inhibition could be present, but be regulated and suppressed if collective migration required it.

This second possibility can be studied in the collectively migrating leading-edge mesendoderm (LEM) of the *Xenopus* gastrula. LEM cells show contact inhibition on artificial *in vitro* substrata. However, when translocating on their endogenous substratum as tight cell aggregates, all cells in contact with the substratum form lamellipodia that are oriented towards the animal pole of the embryo (Winklbauer and Nagel, 1991; Winklbauer and Selchow, 1992; Winklbauer et al., 1992). In the present work, we ask how contact inhibition of lamellipodia is established in LEM cells, how it is suppressed during collective migration, and how this suppression is related to LEM directional migration.

The LEM migrates on the ectodermal blastocoel roof (BCR), which is covered with an extracellular matrix (ECM) of fibronectin (FN) (Nakatsuji et al., 1985; Winklbauer and Stoltz, 1995; Winklbauer, 1998). FN interacts not only with other matrix components and cellular receptors, but also with itself to assemble into fibrils (Schwarzbauer and DeSimone, 2011). Interaction with the FN fibrils of the BCR, or with an artificial substratum of purified FN, is necessary and sufficient for lamellipodia formation in isolated LEM cells (Winklbauer, 1990; Winklbauer and Selchow, 1992; Ramos and DeSimone, 1996; Wacker et al., 1998; Luu et al., 2008). However, on pure FN, contact leads to the sudden retraction of lamellipodia in colliding LEM cells, which might explain the absence of protrusions inside LEM cell aggregates on FN (Winklbauer et al., 1992). The presence of lamellipodia in the embryo and in LEM aggregates migrating on BCR matrix *in vitro* (Winklbauer et al., 1992) suggests that factors within the matrix block contact inhibition.

Here, we show that a matrix-binding form of platelet-derived growth factor-A (PDGF-A), which is expressed in the BCR and guides LEM migration (Ataliotis et al., 1995; Nagel et al., 2004; Smith et al., 2009; Damm and Winklbauer, 2011), enables cells to overcome contact inhibition of lamellipodia. Contact inhibition is implemented in LEM cells through a control module that includes the FN receptor integrin α5β1 and the heparan sulfate proteoglycan syndecan 4. Both factors can bind FN, and we show that FN interaction is indeed involved. However, FN present as puncta on the surface of LEM cells, rather than the FN serving as external substratum for migration, is part of the control module (Winklbauer, 1998). In contrast to the well-studied FN fibrils, little is known about this cell surface FN (csFN). The most detailed description of its function so far relates to the dissemination of rat breast cancer: csFN puncta mediate attachment of the cancer cells to lung endothelium,

University of Toronto, Department of Cell and Systems Biology, 25 Harbord Street, Toronto M5S 3G5, ON, Canada.

*Author for correspondence (r.winklbauer@utoronto.ca)

R.W., 0000-0002-0628-0897

Received 17 December 2017; Accepted 25 May 2018

Development (2018) 145, dev162651. doi:10.1242/dev.162651

which is essential for pulmonary metastasis (Cheng et al., 1998, 2003; Huang et al., 2008).

We show further that the csFN-integrin α5β1-syndecan 4 module is controlled by p21-activated kinase 1 (Pak1) to regulate, in turn, the Eph receptor tyrosine kinase ligand, ephrin B1, which eventually controls lamellipodial stability. Thus, the external FN substratum permits LEM cells to form lamellipodia; Pak1 acts through the csFN-integrin-syndecan module on ephrin B1 to induce the collapse of lamellipodia upon contact, implementing a contact inhibition mechanism; and PDGF-A signaling interferes with the control module to overcome inhibition and to stabilize lamellipodia. This stabilization is directional, consistent with a role of PDFG-A signaling in LEM cell orientation and guidance.

RESULTS

LEM cell aggregation inhibits lamellipodia formation on FN substratum

To reconstruct the collective migration of LEM cell aggregates *in vitro*, we first analyzed the contact behavior of single cells on purified FN, the minimal substratum for LEM migration. Free LEM cells translocated on FN while extending two to three lamellipodia, and a protrusion usually collapsed when a cell started to move in the opposite direction (Fig. 1A, Movie 1). During collapse, filopodia extended from the shrinking lamellipodia, to turn eventually into retraction fibers (Fig. 1B). The average lifetime of lamellipodia was 10 min (Fig. 1G). Movement away from an existing lamellipodium was largely prevented when cells were part of an aggregate (Fig. 1E), and lamellipodia protruding from the margin of such an aggregate survived for 35 min on average (Fig. 1G, Movie 2). Nonattached, isolated LEM cells extend protrusions from an active zone, which persists for a similar time (Winklbauer and Selchow, 1992), suggesting that the intrinsic lifespan of LEM protrusions is about 30 min.

When lamellipodia collide head-on with those of other cells, they immediately retract (Winklbauer et al., 1992). We observed that lamellipodia also collapsed when they underlapped a cell body (Fig. 1C). Small protrusions shrank and vanished, whereas larger ones retreated between filiform extensions that rapidly protruded, as though the lamellipodium were transiently changing into a bundle of filopodia. Eventually, retraction fibers attached to the target cell surface were left behind as the contacting cell moved away (Fig. 1C). The remaining lifetime after contact was only 1-2 min

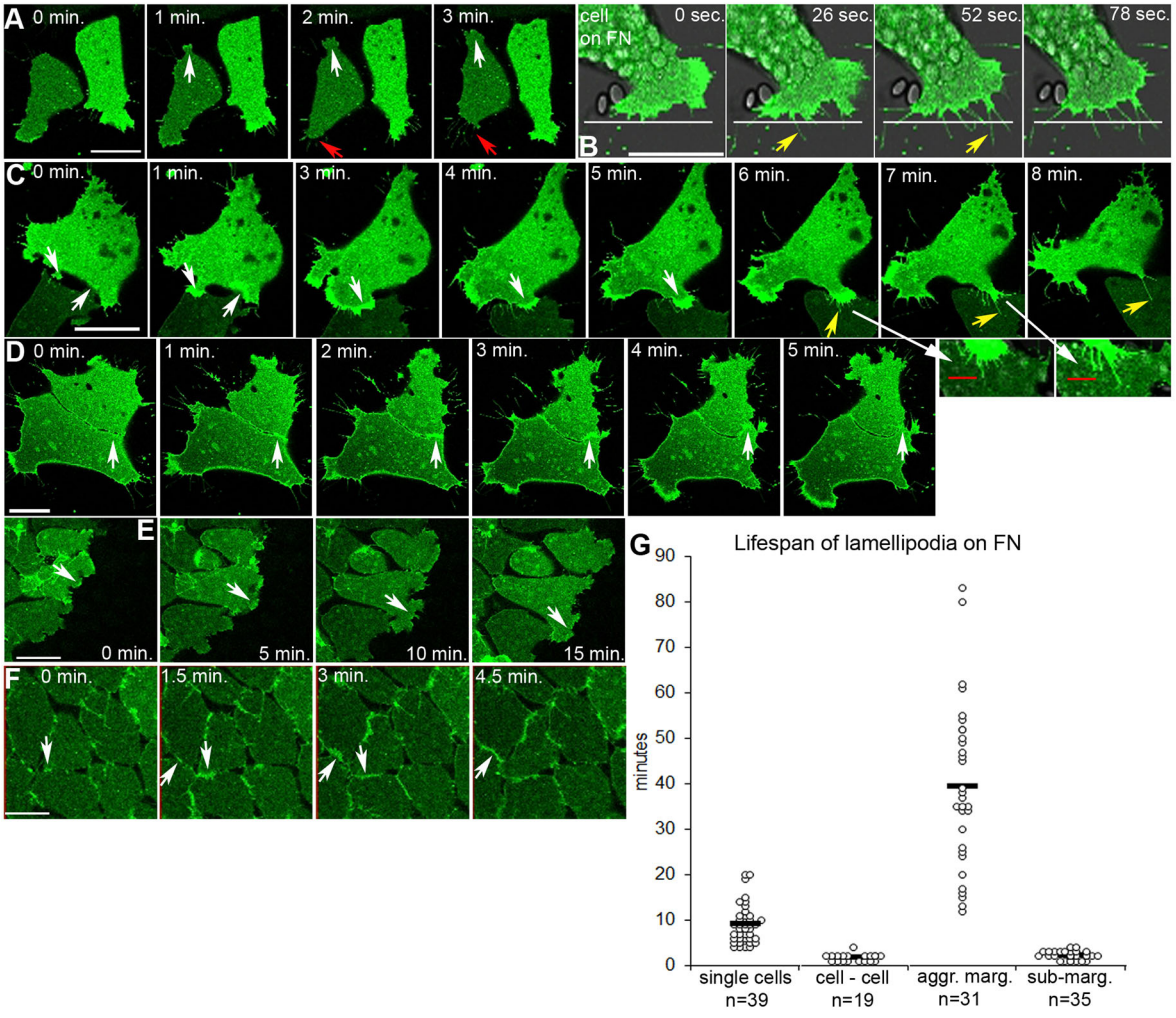

Fig. 1. LEM cell aggregation inhibits lamellipodia formation on FN. (A,B) Isolated LEM cells. White arrows show advancing lamellipodia and red arrows show retracting lamellipodia in all panels. (C) Underlapping of LEM cells. Yellow arrows indicate filopodia emanating from a retracting lamellipodium. Long white arrows point to the magnified view, and red lines show the position of the most advanced filopodium at 7 min. (D) Two LEM cells form small, short-lived lamellipodia at the contact site. (E) LEM aggregate with large lamellipodia at the margin. (F) A LEM aggregate forming a few, small, short-lived protrusions submarginally. All cells are labeled with membrane-GFP. (G) Lifespan of lamellipodia; black bars indicate the mean values. Scale bars: 30 µm.

Development (2018) 145, dev162651. doi:10.1242/dev.162651

(Fig. 1G). Thus, lamellipodia are induced to collapse despite having access to the external FN substratum. The induced retraction appeared similar to not only a Slit-Robo-mediated collapse of growth cones (McConnell et al., 2016), but, notably, also the retraction of free lamellipodia. A basic mechanism of lamellipodia collapse that can be triggered by different molecular or mechanical cues, might be used here in the contact inhibition of lamellipodia.

In apposed cell pairs, tiny processes bridged narrow gaps between cells at different levels above the substratum (Fig. S1A). Directly at the substratum, small lamelliform protrusions of a cell attempted to underlap the adjacent cell, but soon retracted before growing to a significant size (Fig. 1D). As expected from this behavior, protrusion formation was attenuated in the interior of cell aggregates (Fig. 1F). Cells were tightly packed above the substratum level, yet separated by small gaps where attached to FN (Fig. S1B). As in cell pairs, lamelliform protrusions formed, but were small and short-lived because they immediately encountered an adjacent cell and collapsed, turning transiently into bundles of filopodia as they shrunk back and left retraction fibers behind (Fig. 1F). Most of the cells were devoid of lamellipodia at any given time, and the lifetime of protrusions was strongly reduced, to a quarter of that of free lamellipodia (Fig. 1G). Protrusive activity was sustained at the margin, where large lamellipodia extended onto the free substratum surface (Fig. 1E).

Overall, when lamellipodia retracted from a cell body, the short reaction time and narrow range of survival times suggest that the effect of contact is prompt and efficient, and we propose that it corresponds to the first step of a classical ‘contact inhibition of locomotion’. This usually involves a short lamellipodium-to-cell adhesion phase, followed by a retraction of the protrusion (Abercrombie and Dunn, 1975). The second step, where a cell repolarizes and moves away in a different direction, is observed when single LEM cells collide (Winklbauer et al., 1992) but is not expected to occur under the crowded conditions of an LEM cell aggregate.

Expression of kinase-dead Pak1 or knockdown of ephrin B1 prevent contact inhibition of lamellipodia

Expression of kinase-dead Pak1 (KD-Pak1) affects LEM cell protrusions in the embryo (Nagel et al., 2009), and we asked whether it controls lamellipodia stability. In single cells expressing KD-Pak1, lamellipodia were more frequent and larger, and not serrate as in uninjected cells, but smooth-rimmed (Fig. 2A,B). KD-Pak1 induced similar lamellipodia in the interior of LEM aggregates (Fig. 2C,D). Cells were more mobile and less densely packed, with irregular gaps between cells (Fig. S1C, Movie 3). Occasionally, underlapping led to the spontaneous alignment of

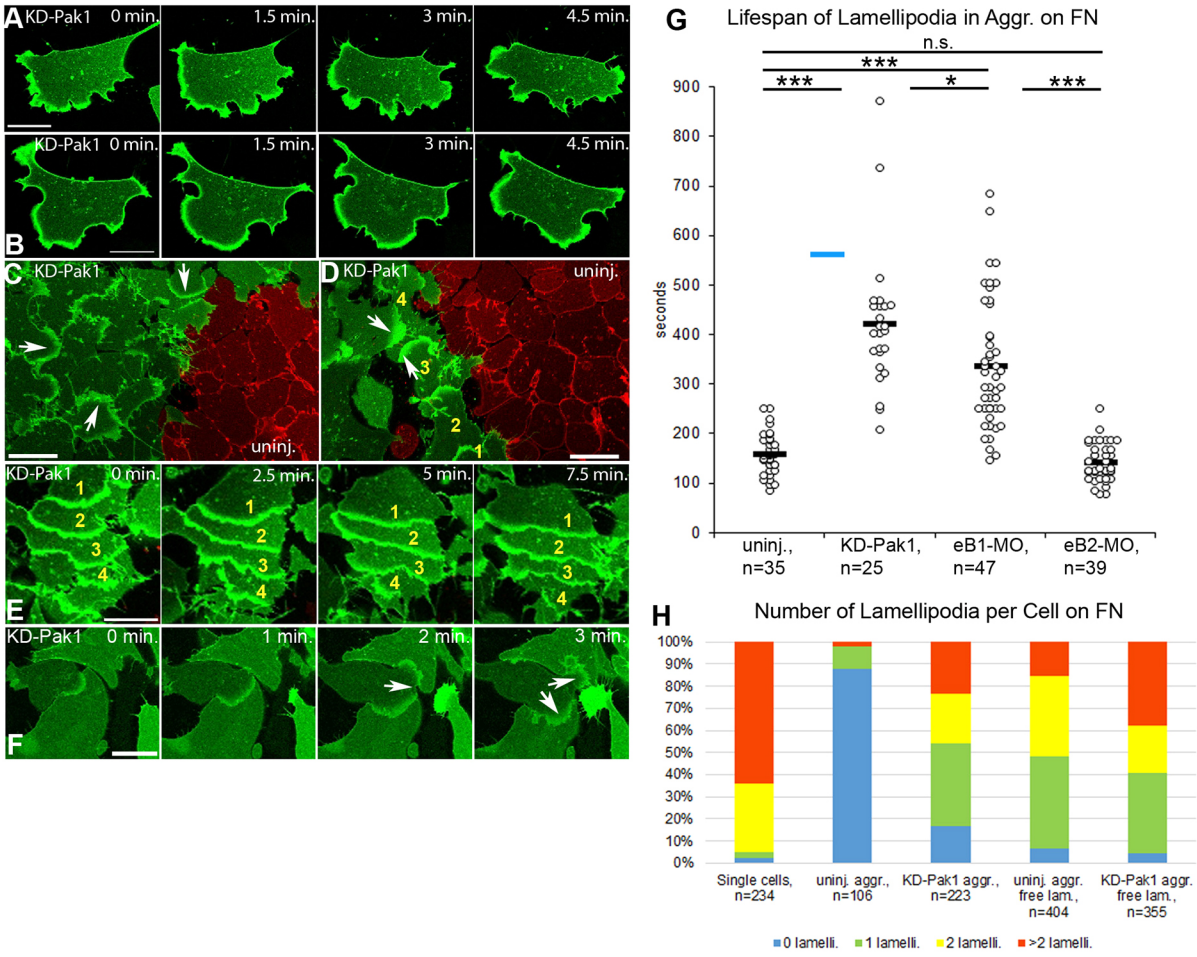

Fig. 2. KD-Pak1 expression overcomes contact inhibition of lamellipodia. (A,B) Isolated LEM cell expressing KD-Pak1 on FN. (C,D) LEM aggregate with KD-Pak1-expressing cells (membrane-GFP, green) and control cells (membrane-RFP, red). White arrows show smooth-rimmed lamellipodia, yellow numbers indicate serially underlapping cells. (E) Time series of oriented underlapping cells (yellow numbers). (F) Lamellipodium splitting in two upon contact (white arrows). (G) Lifespan of lamellipodia. Blue bar indicates mean value of single cells on FN; black bars indicate the mean values. Statistical significance: *P<0.05, ***P<0.0001, n.s., not significant. (H) Percentage of cells having the indicated number of lamellipodia per cell. Scale bars: 30 µm.

Development (2018) 145, dev162651. doi:10.1242/dev.162651

moving cells. A lamellipodium, once under the body of a cell ahead of it, kept this contact and the second cell followed the first one closely. In this way, chains of coordinately moving cells were generated that underlapped each other and pointed in the same direction (Fig. 2E, Movie 4), mimicking the shingle arrangement of directionally migrating LEM cells in the embryo (Winklbauer and Nagel, 1991; Winklbauer and Selchow, 1992; Nagel et al., 2004).

The lifespan of submarginal KD-Pak1-induced lamellipodia was comparable to that of single-cell lamellipodia (Fig. 2G). Protrusions became fragmented when pulled back by respective cell movements and disappeared, while occasionally leaving retraction fibers behind. When two lamellipodia collided, their contacting regions retreated locally, and either they split in two (Fig. 2F) or vanished as a whole. The increased lifetime of KD-Pak1 protrusions (Fig. 2G) contributed to an increased number of lamellipodia per cell (Fig. 2H) and a high protrusion density in aggregates. The number of protrusions per cell at the free margin was not affected (Fig. 2H). Induction of submarginal lamellipodia by KD-Pak1 was also detected by F-actin staining with fluorescent phalloidin, and the effect was reversed by co-expression of constitutively active CA-Pak1 (Fig. S2A-C). Altogether, KD-Pak1 expression induced a new, smooth-rimmed type of lamellipodium and, at the same time, rendered lamellipodia resistant to contact-induced collapse.

Ephrins are also candidates for the promotion of lamellipodial collapse (Astin et al., 2010; Lin et al., 2015). In *Xenopus*, ephrin B1 and B2 are expressed in the mesoderm and are involved in cell repulsion at Brachet's cleft (Rohani et al., 2011). In LEM explants, knockdown of ephrin B1, but not of ephrinB2, strongly stimulated submarginal protrusion formation. Lamellipodia were large and smooth-rimmed, similar to those induced by KD-Pak1, serial underlapping occurred (Fig. 3A, Movies 5 and 6) and lamellipodial lifespans were prolonged (Fig. 2G). Both in KD-Pak1 and ephrin B1-morpholino (MO) aggregates, gaps between cells were wider at the substratum level, but were closed above this level (Fig. S1C-E).

We asked whether ephrin B1 knockdown is required in lamellipodia or the underlapped cell body to stabilize protrusions. In mosaics, lamellipodia of ephrin B1-MO-injected cells were stable not only when in contact with ephrin B1-MO cells, but also when underlapping uninjected cells (Fig. 3B,F). By contrast, lamellipodia of uninjected cells collapsed when in contact with the bodies of ephrin B1-MO or uninjected cells (Fig. 3C,F). Thus, ephrin B1 appears to act in lamellipodia to induce their collapse. Consistent with this notion, ephrin B1 protein is expressed in lamellipodia of single cells (Fig. 3D). However, not all lamellipodia were labeled, and cells appeared polarized with regard to ephrin B1 expression. When mCherry-tagged ephrin B1 (Wen and Winklbauer, 2017) was overexpressed in LEM cells, most lamellipodia were unstable on FN (Fig. 3E). When encountering a cell body, they collapsed after initial spreading, as in control cells: filiform protrusions extended, whereas the lamellipodium shrunk. Retraction fibrils remained behind when the protrusion eventually retreated (Fig. 3F), showing that substratum attachment was not abolished by ephrin B1 overexpression.

Characterization of csFN on LEM cells

Lamellipodia formation in LEM cells depends on an external FN substratum. To see whether csFN also affects lamellipodia stability, we first characterized its presence on LEM cells. Antibody staining

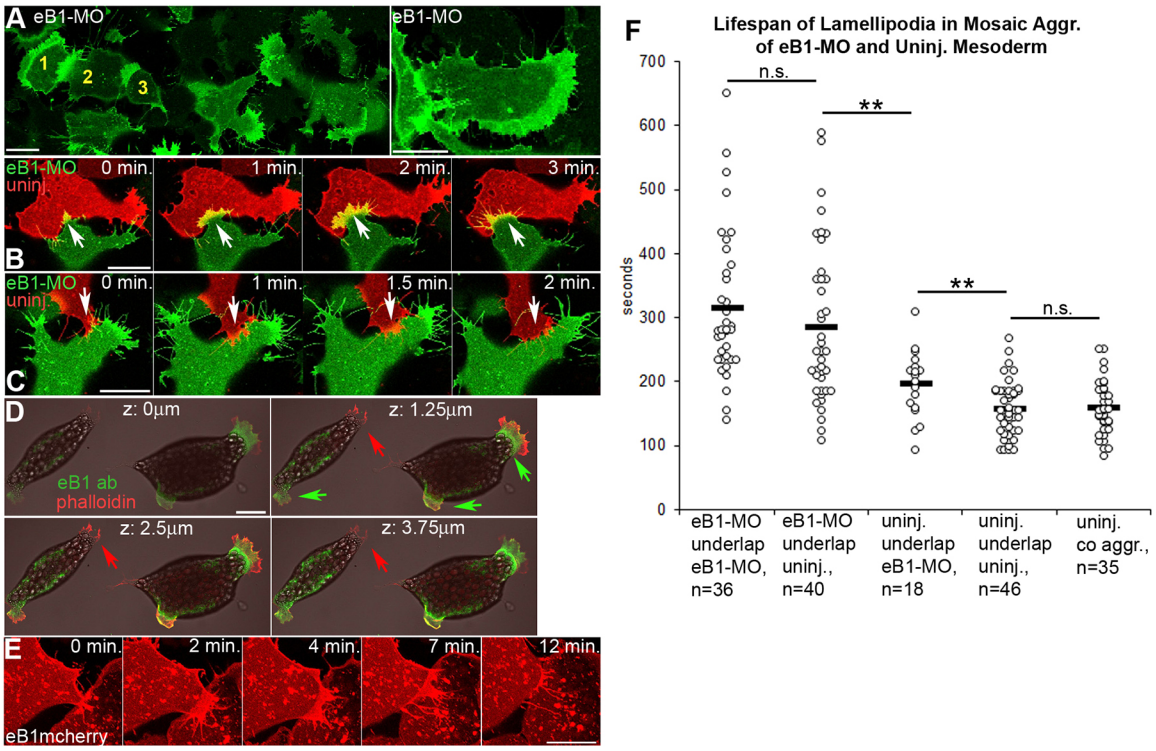

Fig. 3. Ephrin B1 knockdown overcomes contact inhibition of lamellipodia. (A) eB1-MO-injected LEM aggregates form lamellipodia submarginally. Yellow numbers indicate serially underlapping cells. (B,C) Mosaic of eB1-MO-injected (membrane-GFP, green) and control cells (membrane-RFP, red). (B) eB1-MO cell underlaps uninjected cell. (C) Uninjected cell underlaps eB1-MO cell. White arrows indicate underlapping lamellipodia. (D) Immunofluorescence staining with eB1 antibody and secondary antibody (green), and phalloidin counterstaining (red), *z*-stack. Red arrows indicate lamellipodium without eB1 protein, green arrows indicate lamellipodia with eB1. (E) Underlapping of eB1-mCherry-overexpressing cells. (F) Lifespan of lamellipodia in mosaic aggregates. Black bars indicating the mean values. Statistical significance: $^{**}P<0.001$, n.s., not significant. Scale bars: 30 µm.

Development (2018) 145, dev162651. doi:10.1242/dev.162651

showed that, on the surface of LEM aggregates, cells were covered with fine, submicron-sized csFN puncta (Fig. 4A). These puncta were also present at the interface between closely apposed cells within aggregates (Fig. 4B), and at free cell surfaces at interstitial gaps (Fig. 4C). An average-sized lamellipodium covered several puncta (Fig. 4D,D′).

After injection of MO (FN1-MO and FN2-MO) directed against the two isoforms of *Xenopus* FN, the number of FN puncta was strongly reduced, and some cells completely lacked puncta (Fig. 4E,F). Average FN staining intensity was lowered to 37% of controls (Fig. 4G). Integrin α5β1 is the main FN receptor of the gastrula (Whittaker and DeSimone, 1993), and knockdown of the β1 subunit reduced FN staining intensity (Fig. 4G-I). Another putative FN-binding protein, the transmembrane heparan sulfate proteoglycan syndecan 4, is ubiquitously expressed in the embryo, and required for gastrulation (Muñoz et al., 2006) and for the development of the LEM-derived foregut (Zhang et al., 2016). Its knockdown with MO (xSyn4.1-MO and xSyn4.2-MO) directed against the two *Xenopus* isoforms reduced syndecan 4 expression (Fig. 4G) but did not affect csFN density or distribution

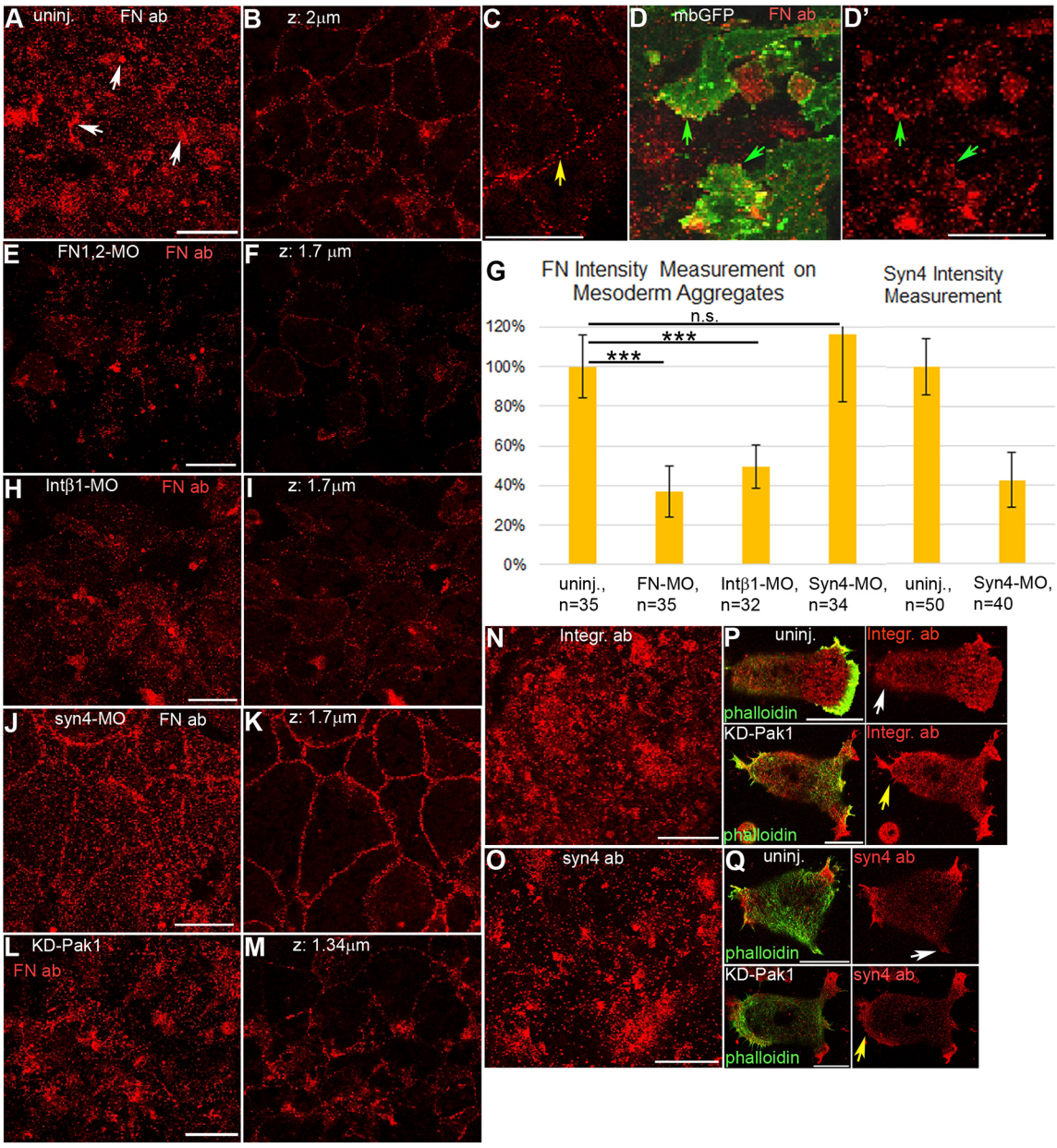

Fig. 4. Characterization of csFN on LEM cells. (A-M) LEM aggregates stained with antibody against *Xenopus* FN. (A-C) Immunofluorescence images show small csFN puncta and clusters of puncta (white arrows) on the free cell surfaces (A) and puncta between cells within the aggregate (B). (C) Yellow arrow points to free cell surfaces at interstitial gap in an aggregate, with csFN puncta on each surface. (D,D′) Lamellipodia (membrane-GFP) (green arrows) cover several csFN puncta (red). (E,F) Knockdown of FN by FN1,2-MO reduces FN puncta on the surface of the aggregate (E) and between cells (F). (G) Intensity of csFN antibody staining was measured on the cell surfaces of the aggregates, using Leica LAS AF Lite software. The average fluorescence intensity of csFN of uninjected aggregates was set to 100%. (H-K) csFN staining after integrin β1 knockdown (H,I) or syndecan 4 knockdown (J,K) on the LEM surface (H,J) or between cells (I,K). (L,M) csFN staining of KD-Pak1-expressing cells on the LEM surface (L) or between cells (M). (N,O) Immunofluorescence staining of LEM explant surface with antibody against integrin β1 (N) or syndecan 4 (O). (P,Q) Double staining with fluorescent phalloidin and integrin β1 (P) or syndecan 4 (Q) antibodies in KD-Pak1-expressing or -nonexpressing cells. Scale bars: 30 μm.

Development (2018) 145, dev162651. doi:10.1242/dev.162651

(Fig. 4G,J,K). Similarly, KD-Pak1 expression did not alter the csFN pattern (Fig. 4L,M).

Compared with the punctate FN staining, integrin β1 distribution was more diffuse (Fig. 4N). Syndecan 4 expression was punctate, but patches were larger and fewer compared with csFN puncta (Fig. 4O). Thus, neither of the two putative receptors for csFN showed an expression pattern identical to that of csFN, but integrin function was required for csFN puncta formation or retention, whereas syndecan 4 was dispensable. Although KD-Pak1 expression did not affect the csFN distribution on cell bodies, it increased the lamellipodial localization of integrin β1 and syndecan 4 in single cells (Fig. 4P,Q).

csFN, integrin α5β1 and syndecan 4 regulate contact-induced lamellipodia collapse

Knockdown of csFN with FN-MOs had no effect on the shape or lifetime of submarginal lamellipodia (Fig. S3A,B). In LEM aggregates co-injected with KD-Pak1 mRNA and FN-MOs, cells formed broad, smooth-rimmed submarginal lamellipodia, as expected from KD-Pak1 cells. However, lamellipodia collapsed consistently and rapidly, switching transiently to filopodia extension before retreating and leaving retraction fibers behind (Fig. 5A,F, Movie 7). Marginal lamellipodia were stable (Fig. 5B), indicating that external FN substratum could be used in csFN-depleted aggregates, but that it was not able to stabilize submarginal protrusions: csFN was required to overcome contact inhibition of lamellipodia. In FN-MO/KD-Pak1 cells, ephrin B1-MO fully rescued lamellipodia stability (Fig. 5C,F), placing csFN function upstream of ephrin B1 and downstream of Pak1 (Fig. 5G).

Given that csFN density is reduced upon integrin β1 knockdown, we asked whether the latter treatment also interfered with lamellipodia stabilization. Surprisingly, in KD-Pak1-expressing aggregates, knockdown of integrin β1 did not shorten lamellipodial lifespans (Fig. 5F). In fact, injection of integrin β1-MO alone promoted submarginal lamellipodia (Fig. 5D,F), and knockdown of integrin β1 in FN-MO explants also increased lamellipodial stability (Fig. 5F). These results imply that integrin interferes with lamellipodia stability, but that it is negatively regulated by FN (Fig. 5G).

Integrin α5β1 recognizes the RGD cell-binding site in FN, and an inhibitory RGD peptide prevents mesoderm cell spreading on FN *in vitro* (Winklbauer, 1990). This raises the question of how lamellipodia can be maintained in integrin β1-MO explants. We noted that single LEM cells extended lamellipodia on FN *in vitro* and migrated even when integrin β1 was knocked down. Interestingly, the smooth-rimmed shape of their protrusions conformed to that of KD-Pak1 or ephrin B1 (eB1)-MO-induced submarginal lamellipodia (Fig. S4). RGD peptide inhibited the spread of both uninjected and integrin β1-MO-injected cells (not shown). It might be that residual integrin α5β1 in the morphants is sufficient for spreading on external FN, but not for a role related to csFN. Alternatively, a different RGD-binding integrin is used in a compensatory manner, for example integrin αvβ3, the subunits of which are expressed in the gastrula (Whittaker and DeSimone, 1993).

In contrast to integrin β1-MO, syndecan 4 MOs, which, by themselves, had no effect on lamellipodia shape or lifetime (Fig. S3C), caused the collapse of lamellipodia in KD-Pak1 explants (Fig. 5F). Moreover, lamellipodia were not smooth-rimmed, but serrate and rich in filopodia. Knockdown of integrin β1 in syndecan 4 morphants did not prolong lamellipodia lifespan, suggesting that syndecan 4 acts downstream of integrin. By contrast, ephrin B1-MO increased lamellipodia stability in syndecan 4 morphants (Fig. 5F). Together with a similar effect of ephrin B1-MO in FN morphants, this places a tentative FN-integrin-syndecan module between Pak1 and ephrin B1 (Fig. 5G). Altogether, with the respective results combined, the control factors can be ordered in a linear epistatic interaction pathway. A step-by-step deduction of the pathway is provided in Fig. S5. Formally, all interactions are inhibitory, implying that components are alternatingly 'on' and 'off' along the pathway. With Pak1 active, ephrin B1 is 'on' and causes lamellipodia to collapse upon contact. KD-Pak1 reverses the on-off states of all components, inactivating ephrin B1 and, thus, stabilizing lamellipodia (Fig. 5G). However, the list of components is contingent and not necessarily complete and, with additional factors, further inhibitory or activating interactions could be introduced (Fig. S5).

C-cadherin modulates contact-induced lamellipodia collapse

C-cadherin is the main cell-cell adhesion molecule in the *Xenopus* gastrula (Kühl and Wedlich, 1996; Winklbauer, 2009). It contributes to the mutual attachment of cells, but it is not clear whether it also mediates the adhesion of lamellipodia to cell bodies. When we knocked down C-cadherin in LEM aggregates on FN with C-cad-MO (Ninomiya et al., 2012), cells were loosely packed at the substratum level, but were densely packed interiorly (Fig. S1F). Submarginal protrusions were serrate and fragmented (Fig. 5E), as in untreated cells, but their lifespans were slightly increased compared with controls (Fig. 5E,F). Strikingly, C-cad-MO rescued lamellipodia survival in aggregates where KD-Pak1-induced protrusions had been inhibited by FN-MO injection (Fig. 5F). Weakened cell-cell contact formation and, hence, reduced ephrin B1 signaling in cadherin-depleted aggregates could be responsible for delayed lamellipodia retraction (Zantek et al., 1999; Hess et al., 2006). In *Xenopus* neural crest cells, PDGF-A/PDGFRα signaling affects contact inhibition of locomotion by promoting N-cadherin expression (Bahm et al., 2017). However, this cadherin isoform is not expressed in gastrula-stage LEM (Kühl and Wedlich, 1996), and C-cadherin might have taken over part of the role of N-cadherin.

PDGF signaling promotes submarginal protrusion formation in LEM aggregates

In the embryo or on conditioned substratum, matrix-bound PDGF-A is required for directional migration and oriented protrusion formation (Nagel et al., 2004). We asked whether PDGF-A also promotes submarginal lamellipodia formation in LEM aggregates. We added heparin to surface-adsorbed FN to interact with its heparin-binding domain, and also added a long form of PDGF-A (lf-PDGF-A), which binds to heparin (Smith et al., 2009; Damm and Winklbauer, 2011). Isolated LEM cells migrated and formed lamellipodia on FN-PDGF substrata (Fig. 6A,B). Lamellipodia were similar to those of KD-Pak1 cells, and readily underlapped other cells (Movie 8). The lifespan of free lamellipodia was similar to that of single cells on pure FN (Fig. 6F).

In aggregates on PDGF-FN, LEM cells showed extensive underlapping of large, smooth-rimmed submarginal lamellipodia, often in shingle arrangements, similar to KD-Pak1-expressing cells (Fig. 6C, Fig. S2D). The lifespans of protrusions were similarly increased (Fig. 6F, Movie 9). Cells appeared loosely packed at the substratum level, but gaps vanished interiorly (Fig. S1G). Submarginal protrusions were suppressed by the PDGFR inhibitor AG1296 and the PI3K inhibitor LY294002 (Fig. S2E,H) on PDGF-FN, but not in KD-Pak1 aggregates on FN (Fig. S2G), consistent with a PDGF signaling-dependent effect (Nagel et al., 2004). Likewise, expression of a kinase-dead PDGF receptor-α

Development (2018) 145, dev162651. doi:10.1242/dev.162651

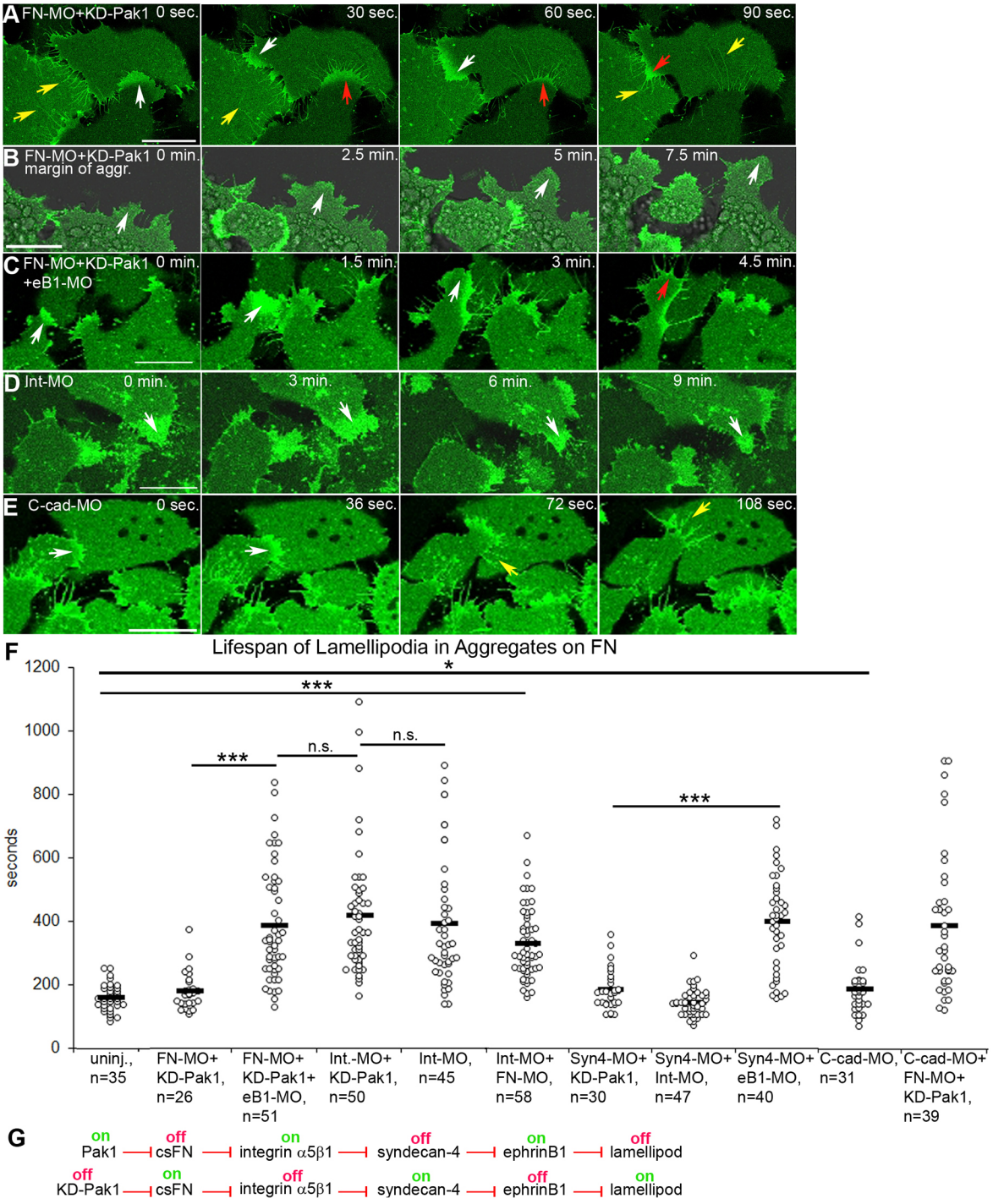

Fig. 5. csFN, integrin α5β1, syndecan 4 and C-cadherin regulate contact-induced lamellipodia collapse. (A-E) Frames from confocal time-lapse movies of LEM aggregates on FN, labeled with membrane-GFP. (A,B) Cells injected with FN-MO, KD-Pak1 mRNA and mbGFP mRNA, (A) submarginal region, (B) explant margin. Yellow arrows point to filopodia, white arrows point to advancing lamellipodia, and red arrows point to retracting lamellipodia in all panels. (C) LEM aggregates injected with FN-MO, KD-Pak1 mRNA and eB1-MO. LEM aggregates injected with (D) integrin β1-MO or (E) C-cadherin-MO. (F) Lifespan of lamellipodia. Black bars indicate the mean values. Statistical significance: **P*<0.05, ***P*<0.001, ****P*<0.0001, n.s., not significant. (G) Pathway deduced from experiments. Scale bars: 30 µm.

(KD-PDGFRα), which interferes with PDGF-A signaling in LEM cells (Nagel et al., 2004), diminished submarginal protrusion formation (Fig. 6D,F).

To see whether PDGF signaling affected contact inhibition by rendering cells nonrepulsive or lamellipodia nonresponsive, we generated mosaics of untreated and KD-PDGFRα-expressing LEM cells and observed contact behavior on FN-PDGF (Fig. 6E). Under these conditions, untreated cells underlapped each other, and lamellipodia survived as in untreated explants. However, lamellipodial lifetime was shortened when KD-PDGFRα cells underlapped untreated cells, untreated cells moved underneath KD-PDGFRα cells, or KD-PDGFRα cells moved under

Development (2018) 145, dev162651. doi:10.1242/dev.162651

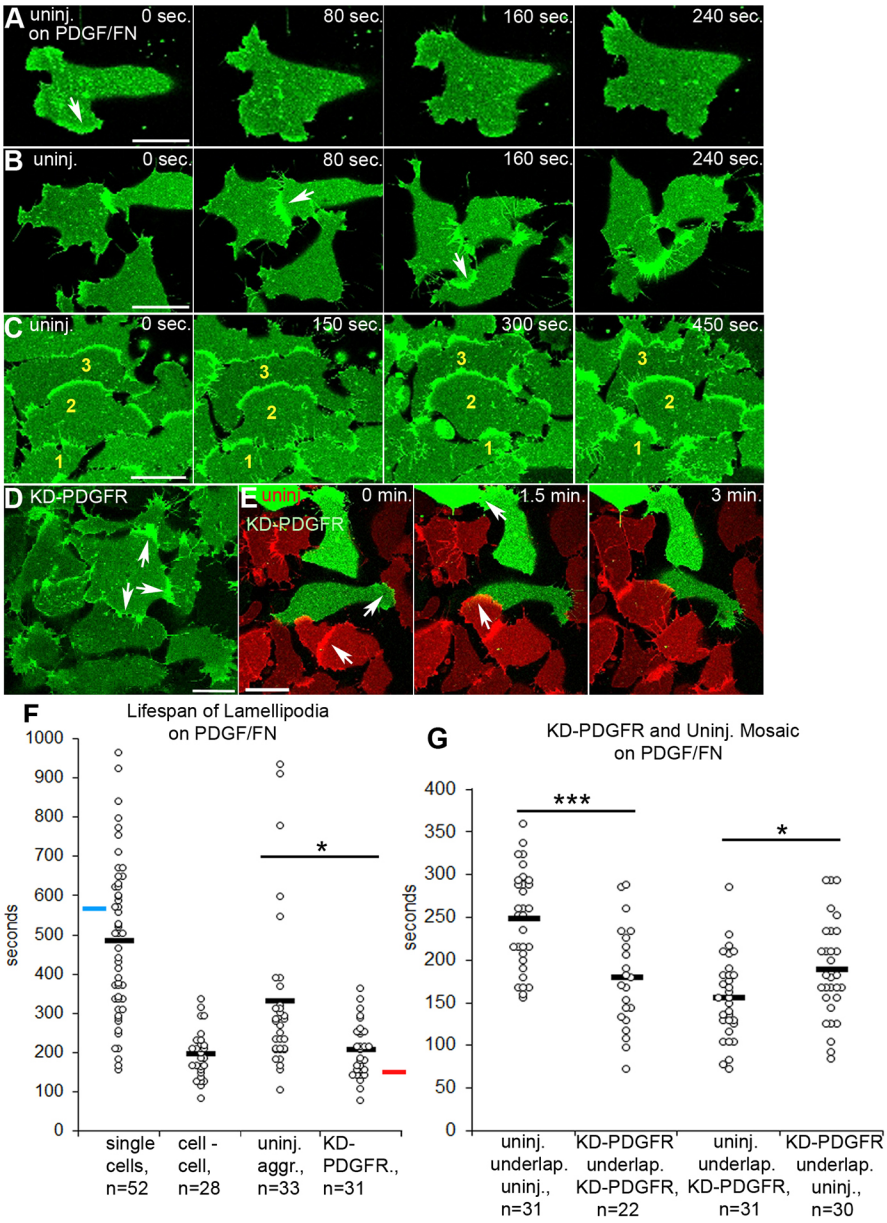

Fig. 6. PDGF signaling promotes submarginal protrusion formation in LEM aggregates. (A-E) Frames from time-lapse recordings of membrane-GFP-labeled LEM cells on PDGF-FN. (A,B) Single cells, white arrows show lamellipodia. (C) Serial underlapping of lamellipodia (yellow numbers) in LEM aggregate. (D) KD-PDGFR-expressing aggregates exhibiting small, nonaligned lamellipodia (white arrows). (E) Mosaic of control (membrane-RFP, red) and KD-PDGFR-expressing cells (membrane-GFP, green). White arrows indicate underlapping lamellipodia. (F,G) Lifespan of lamellipodia on PDGF-FN. Black bars indicate mean values, blue bar indicates mean for single cells on FN, red bar indicates mean for aggregates on FN. Significance: *P<0.05, ***P<0.0001. Scale bars: 30 µm.

KD-PDGFRα cells (Fig. 6G). Thus, PDGF-A signaling is required in both of two interacting cells to prevent lamellipodial collapse.

PDGF signaling acts on the FN-integrin-syndecan module to stabilize protrusions

The similarity of the effects of KD-Pak1, ephrin B1-MO and PDGF-A suggests that the Pak1-ephrin B1 axis normally destabilizes submarginal lamellipodia, and that PDGF-A signaling overcomes this inhibition of protrusion maintenance. To place PDGF-A relative to Pak1, we expressed constitutively active CA-Pak1 in the LEM. In such aggregates, long-lived submarginal protrusions formed on PDGF-FN (Fig. 7A,F), consistent with PDGF-A acting downstream of Pak1. In agreement with this, DN-Pak1 augmented lamellipodia formation on FN-PDGF (Fig. S2F).

Consistent with a requirement of the PDGF signal between Pak1 and ephrin B1, syndecan 4 knockdown reduced lamellipodial lifetimes on PDGF-FN to control levels, and simultaneous eB1 knockdown rescued lamellipodia stability (Fig. 7B,C,F). Integrin β1-MO did not affect protrusion stability on PDGF-FN (Fig. 7D,F). This suggests that PDGF-A signaling acts by inhibiting integrin activity, a function that is performed by csFN in KD-Pak1 cells. As predicted from this interpretation, knockdown of csFN did not interfere with lamellipodia stability on PDGF-FN (Fig. 7E,F). Thus, Pak1 activity indirectly prevents syndecan 4 from inhibiting ephrin B1 (Fig. 5G). PDGF-A signaling blocks this syndecan-inhibiting function and, consequently, syndecan 4 inhibits ephrin B1 and prevents lamellipodial collapse (see Fig. 10A).

PDGF signaling controls protrusion frequency in the embryo

PDGF-A controls the orientation of LEM cell lamellipodia towards the animal pole of the embryo (Nagel et al., 2004). We asked whether it also stabilizes protrusions on the FN fibril matrix of the BCR. LEM migration cannot be observed at high resolution *in situ*, and we examined lamellipodia by scanning electron microscopy (SEM) instead. We confirmed the 'shingle arrangement' of LEM cells (Winklbauer and Nagel, 1991) and identified chains of cells underlapping with wide lamellipodia, as observed in aggregates on PDGF-FN *in vitro* (Fig. 8A). When the matrix-binding lf-PDGF-A

Development (2018) 145, dev162651. doi:10.1242/dev.162651

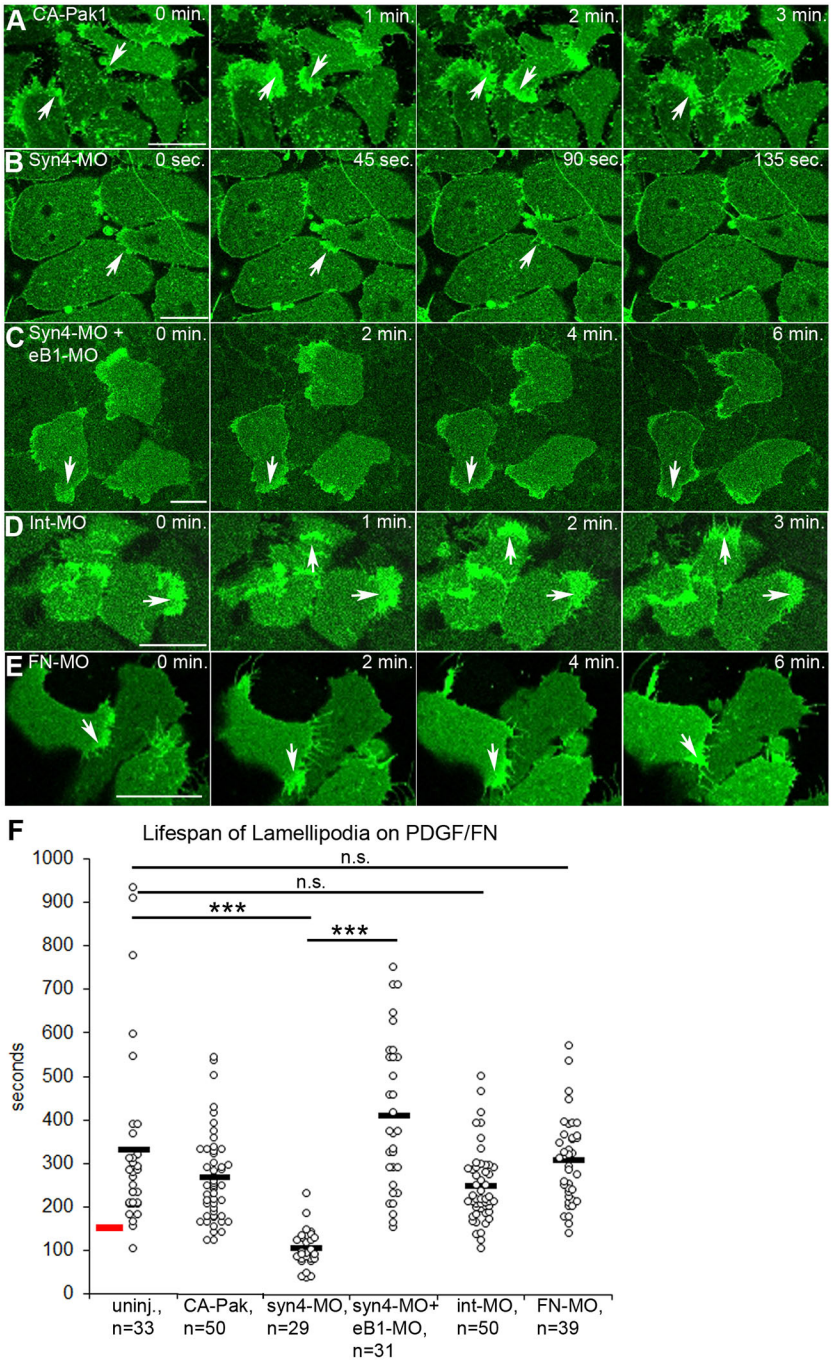

Fig. 7. PDGF signaling replaces the csFN function to control protrusion stability. (A-E) Frames from time-lapse recordings of membrane-GFP-labeled LEM cell aggregates on PDGF-FN substratum. (A) Aggregates expressing CA-Pak1. White arrows indicate lamellipodia in all panels. (B) Syndecan 4-knockdown, small, short-lived lamellipodium. (C) Syndecan 4 and eB1-knockdown lamellipodia. (D) Integrin β1-knockdown lamellipodia. (E) Fibronectin-knockdown lamellipodia. (F) Lifespan of lamellipodia on PDGF-FN. Black bars indicate mean values, red bar indicates mean value of aggregates on FN. Statistical significance: ***P<0.0001, n.s., not significant. Scale bars: 30 µm.

was overexpressed in the BCR, the fraction of cells with two or more lamellipodia increased compared with untreated embryos (Fig. 8B,D), and protrusions were disoriented (Fig. 8B), as shown previously (Nagel et al., 2004). By contrast, dominant-negative PDGF-A increased the fraction of cells with no protrusions, and remaining lamellipodia were small and serrate (Fig. 8C,D). These findings are consistent with PDGF-A stabilizing lamellipodia in LEM cells in the embryo. Pak1 polarizes single LEM cells *in vitro* by constraining the size and the number of lamellipodia per cell (Nagel et al., 2009); in addition, it promotes the contact-induced collapse of lamellipodia. In the embryo, KD-Pak1 expression increases the number of lamellipodia per cell, and the normal number is rescued by co-expression of Pak1 (Fig. 8D). Both functions of Pak1 in LEM cells could contribute to this effect.

In the *Xenopus* gastrula, PDGF-A is expressed in the BCR, and its receptor, PDGFRα, in the mesoderm (Ho et al., 1994). Interestingly, PDGFRα protein expression is polarized in LEM cells *in situ* (Fig. 8E). The receptor forms puncta on the LEM cell surface that are larger yet fewer than those of integrin β1 and are evenly distributed over much of the cell surface. However, puncta are concentrated into dense patches at animally oriented protrusion and are occasionally also enriched at the animally oriented sides of cells in the absence of protrusions. Integrin β1 is also dense at protrusions, but, although it overlaps, it is not strictly colocalized with PDGFRα (Fig. 8E,F). Protrusions pointing laterally do not accumulate the receptor (Fig. 8F). Likewise, single LEM cells on FN or on PDGF-FN do not enrich the receptor at or near lamellipodia (Fig. 8G,H), suggesting that the effect in the embryo results from orienting cues in the BCR matrix.

Development (2018) 145, dev162651. doi:10.1242/dev.162651

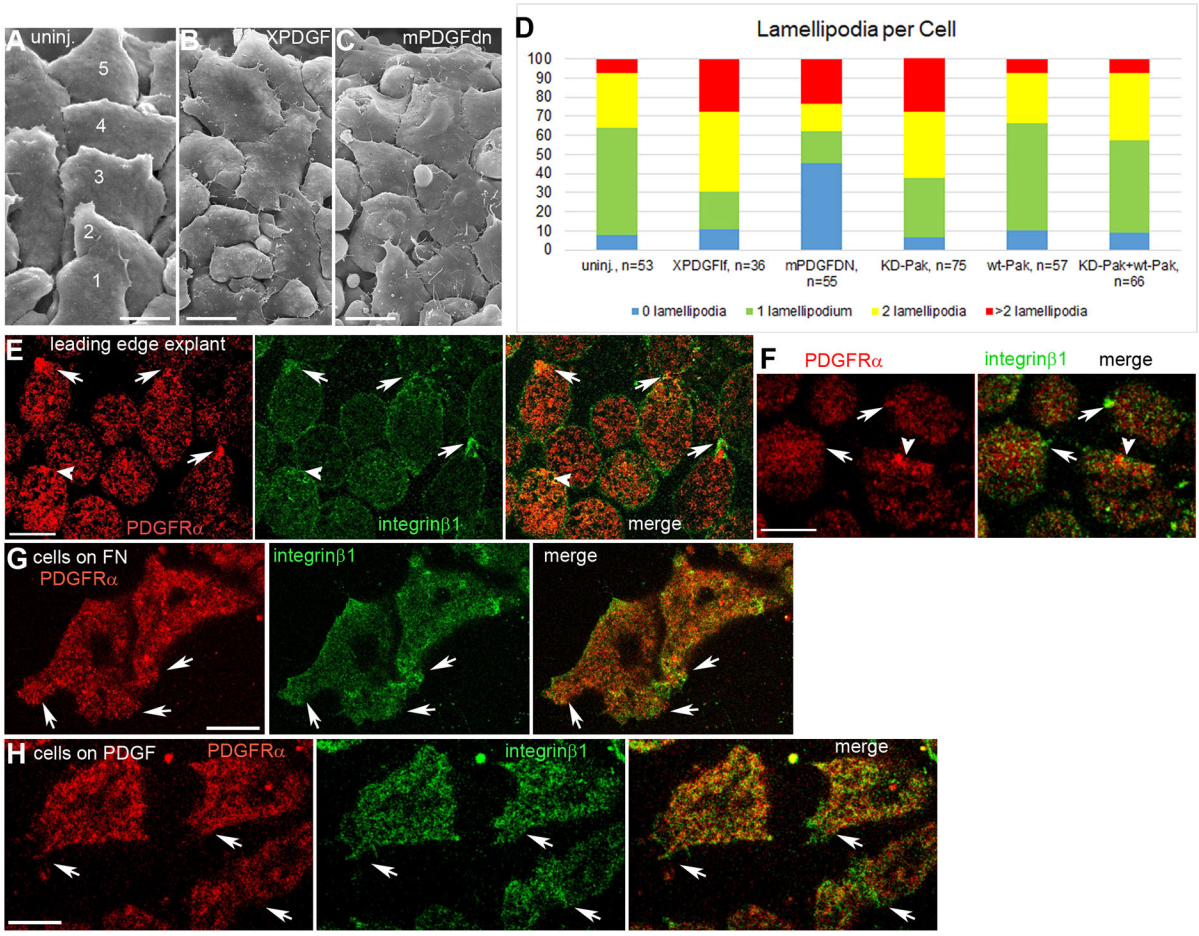

Fig. 8. PDGF-A signaling controls protrusive activity in the embryo. (A-C) SEM images of the substratum-facing surface of the LEM after removal of the BCR of uninjected (A), matrix-binding *Xenopus* lf-PDGF-A (B), and dominant-negative mouse mPDGF-A (C)-expressing gastrulae. (D) Lamellipodia per cell under different experimental conditions, as determined from SEM images. (E,F) Formerly substratum-attached surface of LEM double-stained with PDGFRα (red) and integrin β1 (green) antibodies. Arrows indicate protrusions, whereas arrowheads indicate receptor accumulations in absence of protrusions. (G,H) Single LEM cells on FN (G) or PDGF-FN (H) double-stained for PDGFRα (red) and integrin β1 (green). Arrows indicate protrusions. Scale bars: 30 µm.

PDGF signaling directionally stabilizes protrusions on the *in vivo* substratum

To directly observe the effects of matrix-bound PDGF-A, we examined LEM cells migrating directionally on the endogenous FN- and PDGF-A-containing ECM deposited *in vitro* by cultured BCR (Fig. 9A) (Nagel et al., 2004). On this conditioned substratum, LEM aggregates formed submarginal protrusions similar to those on PDGF-FN, although they were narrower and more serrate (Fig. 9B), perhaps because FN is present as discrete fibrils rather than as an even layer. Most cells extended one protrusion (Fig. 9D) in animal orientation (Fig. 9E), and the lifetime of lamellipodia was prolonged, as on PDGF-FN (Fig. 9F). The shape and size (Fig. 9C), frequency (Fig. 9D), orientation (Fig. 9E) and lifetime of lamellipodia (Fig. 9F) were all sensitive to treatment with the PDGFR inhibitor AG1296, confirming that both the stabilization and orientation of protrusions depend on PDGF-A present in the BCR matrix.

We next asked whether protrusions are stabilized and oriented by two parallel PDGF functions, or whether orientation comprises the selective stabilization of lamellipodia pointing animally. Indeed, in LEM explants on conditioned substratum, lamellipodia that pointed animally survived longer compared with protrusions pointing vegetally, which collapsed rapidly (Fig. 9G). Together with the polarized expression of the PDGF receptor, this suggests that, on conditioned substratum, PDGF-A stabilizes lamellipodia in an oriented fashion.

DISCUSSION

Integrins, cadherins and Eph/ephrin signaling have previously been implicated in contact inhibition of locomotion (see below). Concentrating on lamellipodial collapse as an essential component of contact inhibition, and by adding Pak1, syndecan 4 and csFN to the system, we were able to formally order these disparate factors in an epistatic interaction framework. Moreover, we found that PDGF-A signaling constitutes a branch of this network that relieves contact inhibition to increase lamellipodial lifetimes in aggregates (Fig. 10A). On the endogenous substratum of LEM migration, the PDGF-A-containing BCR matrix, lamellipodia stabilization was directionally biased, linking the contact inhibition-suppressing function of PDGF-A to its role in LEM guidance.

An integrin-centered control module for contact inhibition of lamellipodia

A role of integrins in contact inhibition of locomotion was first proposed two decades ago, based on observations that ectopic expression in myoblasts of integrin α5, integrin β1 or integrin effectors, such as paxillin and FAK, caused lamellipodial paralysis upon cell contact (Huttenlocher et al., 1998). In support of such a role for integrins, contact-induced lamellipodia collapse was prevented in LEM cells by integrin β1 knockdown, suggesting that the main FN binding integrin α5β1 of the gastrula

Development (2018) 145, dev162651. doi:10.1242/dev.162651

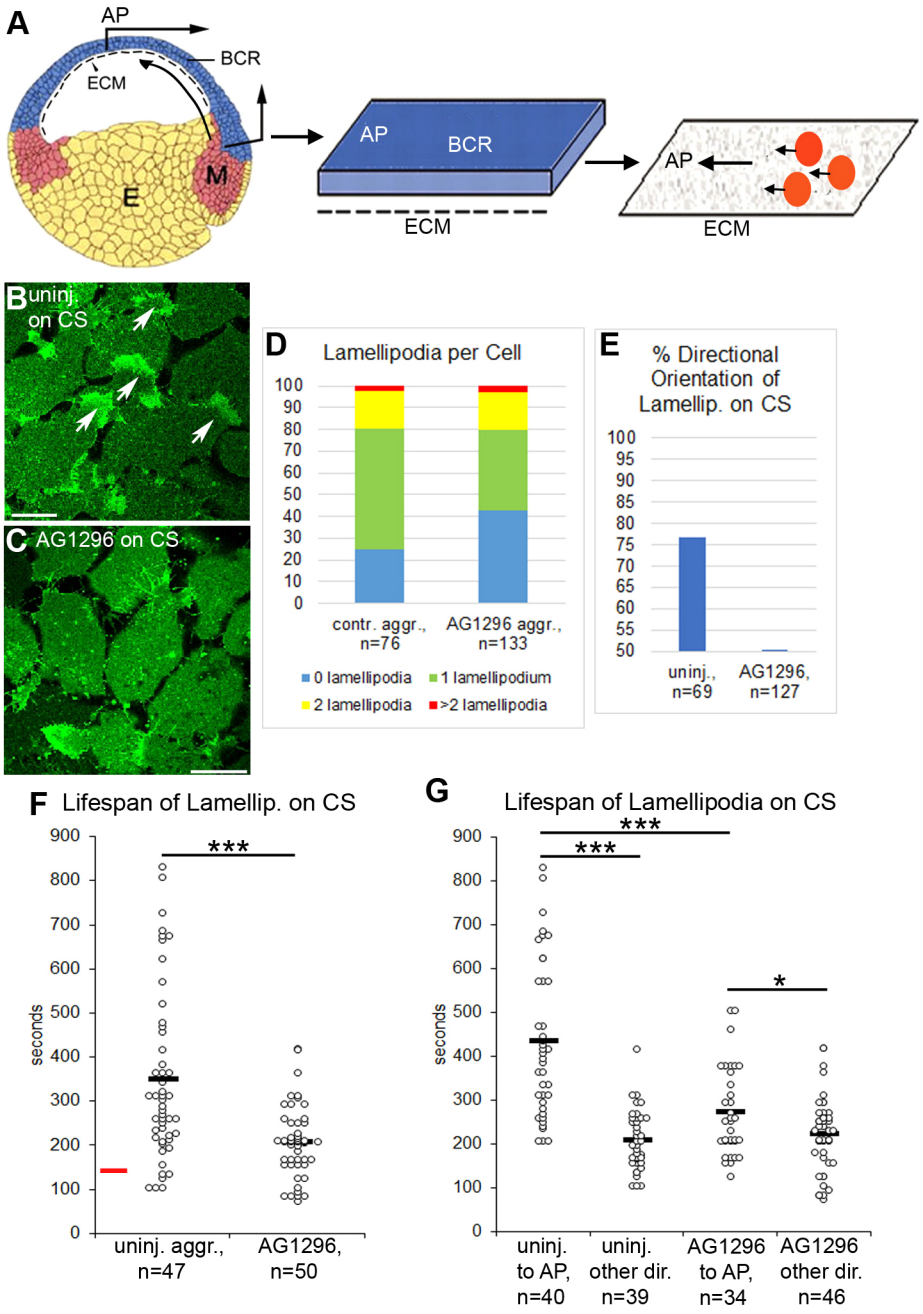

Fig. 9. PDGF-A signaling controls protrusive activity on the endogenous FN matrix substratum. (A) Schematic of substratum conditioning. BCR is placed on the glass bottom of the dish to transfer its ECM. LEM explants (orange) migrate directionally towards the animal pole position (AP). E, endoderm; M, mesoderm. Curved arrow, movement of LEM in embryo. (B,C) Membrane-GFP-labeled LEM aggregates on conditioned substratum without (B) or with PDGFR inhibitor AG1296 (C). Arrows indicate lamelliform protrusions oriented towards animal pole (top right). (D-F) Lamellipodia per cell (D), fraction of lamellipodia orientated towards animal pole (E), and lifespan of lamellipodia (F) on conditioned substratum in untreated or AG1296-treated aggregates. Red bar in F indicates average lifespan on FN. (G) Lifespan of lamellipodia pointing animally (to AP; above line perpendicular to animal-vegetal axis) or in other directions (other dir.; along or below this line) in untreated or AG1296-treated LEM aggregates on conditioned substratum. Statistical significance: **P*<0.05, ****P*<0.0001.

(Whittaker and DeSimone, 1993) is involved. Moreover, we identified csFN as an inhibitor of this integrin function. csFN puncta have been ascribed a role in cancer cell adhesion (Cheng et al., 1998, 2003), and have been shown by transmission electron microscopy to physically link adjacent cells (Hedman et al., 1978; Chen and Singer, 1982). We described here a signaling function for csFN puncta. We also identified a putative FN and integrin interactor, syndecan 4 (Roper et al., 2012), as a target for inhibition by integrin α5β1. We combined these factors into a novel pathway module (Fig. 10A; Fig. S5).

Eph/ephrin signaling has been implicated in various roles in the control of contact inhibition of locomotion. In contacts between prostate cancer cells and fibroblasts, ephrinA-stimulated EphA receptors elicit contact repulsion, whereas EphB/ephrinB interaction suppresses it (Astin et al., 2010; Batson et al., 2014). Ephrin B1 also suppresses contact inhibition in glioblastoma cells (Tanaka et al., 2012). By contrast, ephrin B1/EphB3 signaling in breast adenocarcinoma cells promotes contact inhibition (Lin et al., 2015), as do EphA/ephrin A and EphB/ephrin B interactions in Cajal-Retzius neurons (Villar-Cerviño et al., 2013). In the *Xenopus* gastrula, ephrin B1 is involved in cell repulsion at the ectoderm-mesoderm boundary (Rohani et al., 2011). In LEM cells, it acted downstream of the FN-integrin-syndecan module to mediate contact inhibition of lamellipodia (Fig. 10A). It is required in the lamellipodium and could interact with an Eph receptor on an adjacent cell to sense cell-cell contact and trigger repulsion. Candidate receptors in the LEM would be EphB2 and EphB3 (Rohani et al., 2011).

Pak1 function is required in the LEM for its movement across the BCR (Nagel et al., 2009). In the present context, it antagonized

Development (2018) 145, dev162651. doi:10.1242/dev.162651

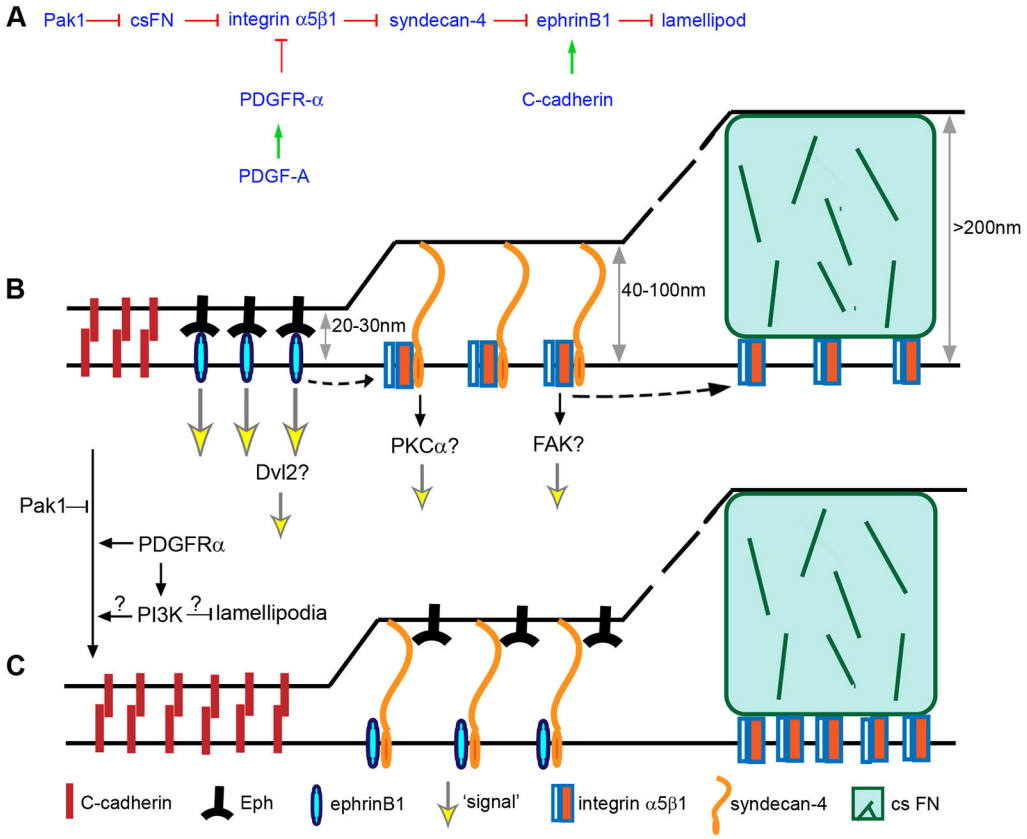

Fig. 10. Control of lamellipodia stability. (A) Epistatic interactions outlining a control network that regulates the cell contact-dependent lifespan of lamellipodia. (B,C) Possible molecular interactions underlying contact inhibition of lamellipodia through ephrin signaling (B) or the absence of contact repulsion (C).

lamellipodia stability by acting upstream of other factors. Based on their epistatic relationships, these factors can formally be placed in an interaction network (Fig. 10A). The central module mediates a series of inhibitory interactions, which implies that alternating pathway nodes are either 'on' or 'off' (Fig. 5G). In aggregates on FN, submarginal lamellipodia collapsed, supposedly because of Pak1 inhibiting the next node in the interaction network, csFN. This notion describes a formal placement of Pak1 in the pathway; the actual interaction between the cytoplasmic kinase and the extracellular FN will of course be indirect. Nevertheless, Pak1 activity determines the on-off state of each pathway component and induces contact inhibition by blocking the inhibition of ephrin B1 (Figs 5G and 10A).

Pak1 inhibition, knockdown of integrin β1 or ephrin B1, and also exposure to PDGF-A not only increased the stability, but also changed the shape of lamellipodia, from serrate and moderate-sized to smooth-rimmed and wide. Importantly, when FN-MO was injected into KD-Pak1 cells, lamellipodia were of the smooth-wide type, but collapsed upon contact, indicating that lamellipodia shape and lifespan are controlled independently. In syndecan 4 morphants, lamellipodia were similar to those of untreated cells, suggesting that syndecan 4 is required for the smooth shape as well as for the prolonged lifetime of protrusions. A similar change in lamellipodia shape in cultured epithelial cells is associated with a transition from integrin α5β1 to integrin αvβ3 (Danen et al., 2005), possibly because of syndecan 4 differential phosphorylation (Morgan et al., 2013). Such a transition would explain the RGD peptide-sensitive, yet integrin β1-independent, migration of LEM cells on FN in our experiments. This transition also implies that the FN-integrin-syndecan module not only regulates lamellipodia-cell body interactions, but also selects integrin α5β1 or integrin αvβ3, depending on its activity status, for adhesion to the external FN substratum.

Interactions of module components

Two types of mechanism could underlie the formally deduced interactions of pathway components: (1) the physical association of components at the membrane in *cis* or *trans*, modulated by the steric exclusion of some associations because of molecular size; and (2) signaling exchanges between the factors involved. To illustrate the first mechanism by a hypothetical example (Fig. 10B,C), we assume a state where a lamellipodia-destabilizing Eph/ephrin *trans*-interaction occurs (Fig. 10B), requiring membrane separation distances close to the 25 nm found at cadherin contacts (Lambert et al., 2005; Xu et al., 2013). Some of the integrin α5β1 molecules are assumed to bind csFN puncta >100 nm in size (Hedman et al., 1978; Chen and Singer, 1982), but others would associate with syndecan 4 (Fiore et al., 2014) and competitively block a putative ephrin-syndecan interaction. In a different state (Fig. 10C), integrins would preferentially bind to csFN, which would allow ephrin B1 to associate with syndecan 4, perhaps through the scaffold protein, syntenin (Grembecka et al., 2006). With a membrane separation distance of >40 nm at syndecan sites (Roper et al., 2012), Eph/ephrin *trans*-interaction would be excluded and signaling would be blocked, allowing lamellipodia to survive cell contact. The first state could depend on Pak1 activity, the second on either its absence, or on the presence of the PDGF-A signal.

The involvement of Pak1, a cytoplasmic kinase, indicates that the second mechanism, interaction by signaling, is involved at least at one point in the pathway, and indirect evidence suggests that integrin inhibition by PDGFRα is also transmitted through the cytoplasm. Moreover, in the previous description of the role of integrin in contact inhibition, signaling through paxillin and FAK was implicated (Huttenlocher et al., 1998). Multiple signaling pathways originate at syndecan 4, for example PKCα-based branches (Roper et al., 2012; Afratis et al., 2017), which could

Development (2018) 145, dev162651. doi:10.1242/dev.162651

indirectly affect ephrin B1 activity. Future analysis must also address the possibility that different components of the mechanism function on different sides of the lamellipodium-cell body contact.

PDGF-A-dependent control of lamellipodia stability and oriented migration

In the embryo or on conditioned substratum, PDGF-A overcame Pak1-dependent contact inhibition by blocking the csFN-integrin-syndecan module at the integrin level (Fig. 8A). Although syndecan 4 can physically bind PDGFRβ to integrin α5β1 (Veevers-Lowe et al., 2011; Tanaka et al., 2014), we propose that, in the present context, the interaction is indirect. While the PDGFRα ligand, PDGF-A, is present on the external substratum, integrin α5β1 must interact with csFN at the cell-cell interface. This implies a transmission of the signal across the cell (e.g. from the lower to the upper side of the lamellipodium to be stabilized). A candidate for the respective signal transduction would be PI3K, which affects directional LEM migration on PDGF-containing matrix (Nagel et al., 2004) and lamellipodial lifetime on PDGF-FN.

The control of lamellipodial stability by PDGF-A is linked to the directionality of LEM migration (Nagel et al., 2004). Previously, a PDGF-A gradient in the BCR matrix had been proposed to orient LEM cells (Nagel et al., 2004), although the gradient had not been demonstrated directly. However, regardless of whether PDGF-A distribution is graded, the leading edge of an aggregate cell at a given animal-vegetal position would encounter the same PDGF-A concentration as the rear end of a cell directly ahead of it. In this situation, the polarization of PDFGR-α expression in LEM cells could explain the selective stabilization of animally pointing lamellipodia. Increased receptor density at animally pointing protrusions would increase PDGF-A signal intensity relative to lateral and rear sides and, thus, differentially increase lamellipodia lifetime. PDFGR-α is not polarized on artificial PDGF-FN substratum, yet lamellipodia are stabilized. This could be simply explained by a lower PDGF-A concentration on the BCR matrix compared with the artificial FN-PDGF substratum. In the absence of PDFGR-α polarization, the matrix PDGF-A density would remain below the threshold for contact inhibition suppression.

Receptor polarization could itself be a response to a putative PDGF-A gradient, as part of a mechanism that augments the reaction to a shallow gradient through a positive feedback loop. Chemoattractant-stimulated polarization has been shown for GABA and BDNF receptors on nerve growth cones (Bouzigues et al., 2007; Guirland et al., 2004), and for the PDGF/VEGF receptor during border cell migration in the *Drosophila* ovary (Janssens et al., 2010). The chains of underlapping LEM cells that form on both nonoriented and oriented substratum suggest that spontaneously polarized cell-cell adhesion also contributes to cell alignment, for example through the polarized expression of ephrin B1 in single cells. Such chains of aligned cells could then be oriented towards the animal pole by the same mechanism as individual cells.

In summary, PDGF-A is involved in the suppression of contact inhibition of lamellipodia in the LEM. Suppression occurs in a polarized manner, which has the ultimate effect of orienting cells towards the animal pole, in the direction of overall LEM migration. Cell orientation based on the differential survival of lamellipodia has also been described for the chick neural crest (Genuth et al., 2018). Similar to LEM cells, chick neural crest cells do not exhibit contact inhibition of migration *in situ*, and a combination of increased formation and differential survival of protrusions pointing in the overall direction of movement effectively polarizes cells throughout the translocating cell stream. The averages and ranges of protrusion lifetimes are also strikingly similar in both systems. If PDFGR-α and PDGF-A are expressed at the chick neural crest as they are in other vertebrates (Hoch and Soriano, 2003), it would be interesting to see whether these cells show contact inhibition of movement in the absence of PDGF-A, for example on FN *in vitro*. This would suggest that differential survival of protrusions by the oriented suppression of contact inhibition is conserved not only as a cellular mechanism, but also molecularly.

MATERIALS AND METHODS

Embryos, micromanipulations and injections

Xenopus laevis embryos from *in vitro* fertilized eggs (Animal Use Protocol 20011765, Bioscience LACC) were dejellied with 2% cysteine in 1/10 Modified Barth's Solution [MBS; 88 mM NaCl, 1 mM KCl, 2.4 mM $NaHCO_3$, 0.82 mM $MgSO_4$, 0.33 mM $Ca(NO3)_2$, 0.41 mM $CaCl_2$, 10 mM Hepes (+NaOH), 1% streptomycin, 1% penicillin, pH 7.4], pH 8.0. Embryos were injected at the four-cell stage in both dorsal blastomeres using a Nanoinject II (Drummond Scientific Company) in 4% Ficoll and cultured at 15°C in 1/10 MBS until the gastrula stage.

Preparation of substrata

Tissue culture dishes (35 mm) with a polymer coverslip bottom from ibidi GmbH were coated with bovine plasma FN (Sigma) at 200 ng/ml, or with 200 ng/ml of FN, 5 µg/ml of heparin and 100 ng/ml of human recombinant PDGF-AA (Calbiochem) (PDGF-FN) for 1 h and saturated with 1 mg/ml of bovine serum albumin (BSA) for 30 min. Substrata were conditioned according to Nagel and Winklbauer (1999): stage-10 BCR explants were held against the bottom of tissue culture dishes for 2 h. After removal of the BCR, substrata were saturated with 1 mg/ml BSA.

Microsurgery

Embryos were staged according to Nieuwkoop and Faber (1967). At gastrula stage 10.5, the vitelline membrane was removed with forceps. Microsurgery was performed in MBS at room temperature under a MZ16F (Leica) stereomicroscope. The LEM was excised, cut into four or five pieces and placed on prepared substrata for imaging. Single cells and mosaics were obtained by dissociating mesendoderm aggregates in Dissociation Buffer [88 mM NaCl, 1 mM KCl, 2.4 mM $NaHCO_3$, 10 mM Hepes (+NaOH), 1% streptomycin, and 1% penicillin (pH 7.4)]. For mosaics, two dissociated populations, as indicated in the text, were mixed and reaggregated in MBS. Operation techniques were as described elsewhere (Winklbauer, 1990; Winklbauer and Schürfeld, 1999).

Constructs, mRNA synthesis and injection

A kinase dead construct of the plasmid pCS2 wild-type *Xenopus* PDGFRα (Ataliotis et al., 1995) was linearized with *Nhe*I and transcribed with T7 polymerase. CS2+mbGFP (a gift from R. Harland, University of California at Berkeley, CA, USA) and mbRFP (a gift from A. Bruce, University of Toronto, ON, Canada) were linearized with *Not*I and transcribed with SP6 polymerase. A kinase-dead mutant K281A of xPak1 (KD-Pak1), a constitutively active Pak1 construct, L98F (CA-Pak1) (Poitras et al., 2003; Bisson et al., 2003) were linearized with *Xba*I and transcribed with T7 polymerase. CS2+memeGFP (a gift from R. Harland) and mbRFP (a gift from A. Bruce) were linearized with *Not*I and transcribed with SP6 polymerase. Plasmid pGHE2 containing the long form of *Xenopus* PDGFA (lf-PDGFA) (Mercola et al., 1988), and pGHE2 harboring a processing defective mutant of mouse PDGFA that acts as a dominant-negative mutant in *Xenopus* (mPDGFdn) (Mercola et al., 1990) were linearized with *Nhe*I and transcribed with T7 polymerase. Embryos were injected at the four-cell stage marginally into the dorsal two blastomeres. See Tables S1 and S2 for the amounts of each mRNA injected per blastomere and details of morpholinos used.

Inhibitors

PDGFR inhibitor AG1296 (Calbiochem) (5 µM) and PI3K inhibitor LY294002 (Calbiochem) (30 µM) were dissolved in DMSO (Sigma-Aldrich)

and used as previously described (Nagel et al., 2004). RGD-peptide H-Gly-Arg-Gly-Asp-Ser-Pro-OH (Calbiochem) was used at 4 mg/ml in MBS as previously described (Winklbauer and Keller, 1996).

Cell labeling

Cells were injected with membrane-GFP or membrane-RFP mRNA to label the cell membrane for live imaging. The closely apposed upper and lower membranes of lamellipodia or filopodia showed these structures as more intensely stained regions, compared with the cell body. The identity of lamellipodia was confirmed by fluorescent phalloidin staining (Fig. S2).

Histology

F-actin was stained in specimens fixed in 4% paraformaldehyde (20 min, 0.01% Triton-X-100 added after 5 min) with Alexa Fluor 488 phalloidin or rhodamine phalloidin (Invitrogen) at 1:100 in PBS/BSA for 20 min. Rabbit antiserum against *X. laevis* plasma FN (Winklbauer, 1998) (1:1000), mouse monoclonal antibody 8C8 against *X. laevis* integrinβ1 (1:6; Developmental Studies Hybridoma Bank, University of Iowa, generated by P. Hausen and V. Gawantka), polyclonal rabbit antibody against syndecan 4 (SDC4) (1:200, TA 314520, Acris, OriGene), and polyclonal rabbit antibody against ephrin-B1 (1:200, A-20, sc-1011, Santa Cruz Biotechnology; Lee et al., 2009), and PDGFRα (1:2000, 3164, Cell Signaling Technology; Bahm et al., 2017) were used. Secondary antibodies were Cy3-goat-anti-rabbit IgG, FITC-goat-anti-rabbit IgG and Cy3-goat-anti-mouse IgG (Jackson ImmunoResearch Laboratories). Staining intensity was measured using the Leica Application Suite X software (free download from Leica). For image collection, an If-SP8-nonresonant confocal microscope (Leica) with 40× immersion oil objective and a Zeiss Axiovert 200M microscope (PlanNeofluar 20× and 40× oil objectives) with Leica Application SuiteX software or AxioVision LE64 software (free download from Zeiss) were used. Data were collected from at least two different batches of embryos for each experiment, and at least three time-lapse recordings (eight on average) per experiment. The *n* in the figures relates to the number of lamellipodia counted. Data were compared using the Student's *t*-test (two-tailed, unequal variances).

Scanning electron microscopy

Embryos were fixed in 2.5% glutaraldehyde/0.1 M sodium cacodylate overnight at 4°C, post-fixed in osmium tetraoxide, and dehydrated in an ethanol/0.1 M cacodylate and ethanol/hexamethyl-disilizane series. Specimens were dried overnight, sputter coated with gold-palladium, and inspected using a Hitachi SU 3500 scanning electron microscope.

Acknowledgements

We thank K. Symes, R. Harland, A. Bruce and T. Moss for reagents.

Competing interests

The authors declare no competing or financial interests.

Author contributions

Conceptualization: M.N., R.W.; Methodology: M.N.; Investigation: M.N.; Writing - original draft: R.W.; Writing - review & editing: M.N., R.W.; Visualization: M.N.; Supervision: R.W.; Project administration: R.W.; Funding acquisition: R.W.

Funding

Funding was provided by the Canadian Institutes of Health Research (MOP-53075).

Supplementary information

Supplementary information available online at
http://dev.biologists.org/lookup/doi/10.1242/dev.162651.supplemental

References

Abercrombie, M. (1979). Contact inhibition and malignancy. *Nature* **281**, 259-262.

Abercrombie, M. and Dunn, G. A. (1975). Adhesions of fibroblasts to substratum during contact inhibition observed by interference reflection microscopy. *Exp. Cell Res.* **92**, 57-62.

Afratis, N. A., Nikitovic, D., Multhaupt, H. A. B., Theocharis, A. D., Couchman, J. R. and Karamanos, N. K. (2017). Syndecans - key regulators of cell signaling and biological functions. *FEBS J.* **284**, 27-41.

Astin, J. W., Batson, J., Kadir, S., Charlet, J., Persad, R. A., Gillatt, D., Oxley, J. D. and Nobes, C. D. (2010). Competition amongst Eph receptors regulates contact inhibition of locomotion and invasiveness in prostate cancer cells. *Nat. Cell Biol.* **12**, 1194-1204.

Ataliotis, P., Symes, K., Chou, M., Ho, L. and Mercola, M. (1995). PDGF signaling is required for gastrulation of Xenopus laevis. *Development* **121**, 3099-3110.

Bahm, I., Barriga, E. H., Frolov, A., Theveneau, E., Frankel, P. and Mayor, R. (2017). PDGF controls contact inhibition of locomotion by regulating N-cadherin during neural crest migration. *Development* **144**, 2456-2468.

Bard, J. B. and Hay, E. D. (1975). The behavior of fibroblasts from the developing avian cornea. Morphology and movement in situ and in vitro. *J. Cell Biol.* **67**, 400-418.

Batson, J., MacCarthy-Morrogh, L., Archer, A., Tanton, H. and Nobes, C. D. (2014). EphA receptors regulate prostate cancer cell dissemination through Vav2-RhoA mediated cell-cell repulsion. *Biol. Open* **3**, 453-462.

Bisson, N., Islam, N., Poitras, L., Jean, S., Bresnick, A. and Moss, T. (2003). The catalytic domain of xPAK1 is sufficient to induce myosin II dependent in vivo cell fragmentation independently of other apoptotic events. *Dev. Biol.* **263**, 264-281.

Bouzigues, C., Morel, M., Triller, A. and Dahan, M. (2007). Asymmetric redistribution of GABA receptors during GABA gradient sensing by nerve growth cones analyzed by single quantum dot imaging. *Proc. Natl. Acad. Sci. USA* **104**, 11251-11256.

Carmona-Fontaine, C., Matthews, H. K., Kuriyama, S., Moreno, M., Dunn, G. A., Parsons, M., Stern, C. D. and Mayor, R. (2008). Contact inhibition of locomotion in vivo controls neural crest directional migration. *Nature* **456**, 957-961.

Chen, W.-T. and Singer, S. J. (1982). Immunoelectron microscopic studies of the sites of cell-substratum and cell-cell contacts in cultured fibroblasts. *J. Cell Biol.* **95**, 205-222.

Cheng, H.-C., Abdel-Ghany, M., Elble, R. C. and Pauli, B. U. (1998). Lung endothelial dipeptidyl peptidase IV promotes adhesion and metastasis of rat breast cancer cells via tumor cell surface-associated fibronectin. *J. Biol. Chem.* **273**, 24207-24215.

Cheng, H.-C., Abdel-Ghany, M. and Pauli, B. U. (2003). A novel consensus motif in fibronectin mediates dipeptidyl peptidase IV adhesion and metastasis. *J. Biol. Chem.* **278**, 24600-24607.

Damm, E. W. and Winklbauer, R. (2011). PDGF-A controls mesoderm cell orientation and radial intercalation during Xenopus gastrulation. *Development* **138**, 565-575.

Danen, E. H. J., van Rheenen, J., Franken, W., Huveneers, S., Sonneveld, P., Jalink, K. and Sonnenberg, A. (2005). Integrins control motile strategy through a Rho-cofilin pathway. *J. Cell Biol.* **169**, 515-526.

Davidson, L. A., Marsden, M., Keller, R. and Desimone, D. W. (2006). Integrin alpha5beta1 and fibronectin regulate polarized cell protrusions required for Xenopus convergence and extension. *Curr. Biol.* **16**, 833-844.

Davis, J. R., Luchici, A., Mosis, F., Thackery, J., Salazar, J. A., Mao, Y., Dunn, G. A., Betz, T., Miodownik, M. and Stramer, B. M. (2015). Inter-cellular forces orchestrate contact inhibition of locomotion. *Cell* **161**, 361-373.

Farooqui, R. and Fenteany, G. (2005). Multiple rows of cells behind an epithelial wound edge extend cryptic lamellipodia to collectively drive cell-sheet movement. *J. Cell Sci.* **118**, 51-63.

Fiore, V. F., Ju, L., Chen, Y., Zhu, C. and Barker, T. H. (2014). Dynamic catch of Thy-1-alpha5beta1+syndecan-4 trimolecular complex. *Nat. Commun.* **5**, 4886.

Genuth, M. A., Allen, C. D. C., Mikawa, T. and Weiner, O. D. (2018). Chick cranial neural crest cells use progressive polarity refinement, not contact inhibition of locomotion, to guide their migration. *Dev. Biol.* S0012-1606(17)30654-1.

Grembecka, J., Cierpicki, T., Devedjiev, Y., Derewenda, U., Kang, B. S., Bushweller, J. H. and Derewenda, Z. S. (2006). The binding of the PDZ tandem of syntenin to target proteins. *Biochemistry* **45**, 3674-3683.

Guirland, C., Suzuki, S., Kojima, M., Lu, B. and Zheng, J. Q. (2004). Lipid rafts mediate chemotropic guidance of nerve growth cones. *Neuron* **42**, 51-62.

Gutzeit, H. O. (1991). Organization and in vitro activity of microfilament bundles associated with the basement membrane of Drosophila follicles. *Acta Histochem. Suppl.* **41**, 201-210.

Hayer, A., Shao, L., Chung, M., Joubert, L.-M., Yang, H. W., Tsai, F.-C., Bisaria, A., Betzig, E. and Meyer, T. (2016). Engulfed cadherin fingers are polarized junctional structures between collectively migrating endothelial cells. *Nat. Cell Biol.* **18**, 1311-1323.

Hedman, K., Vaheri, A. and Wartiovaara, J. (1978). External fibronectin of cultured human fibroblasts is predominantly a matrix protein. *J. Cell Biol.* **76**, 748-760.

Hess, A. R., Seftor, E. A., Gruman, L. M., Kinch, M. S., Seftor, R. E. B. and Hendrix, M. J. C. (2006). VE-cadherin regulates EphA2 in aggressive melanoma cells through a novel signaling pathway: implications for vasculogenic mimicry. *Cancer Biol. Ther.* **5**, 228-233.

Ho, L., Symes, K., Yordán, C., Gudas, L. J. and Mercola, M. (1994). Localization of PDGF A and PDGFR alpha mRNA in Xenopus embryos suggests signalling from neural ectoderm and pharyngeal endoderm to neural crest cells. *Mech. Dev.* **48**, 165-174.

Hoch, R. V. and Soriano, P. (2003). Roles of PDGF in animal development. *Development* **130**, 4769-4784.

Huang, L., Cheng, H.-C., Isom, R., Chen, C.-S., Levine, R. A. and Pauli, B. U. (2008). Protein kinase Cε mediates polymeric fibronectin assembly on the surface of blood-borne rat breast cancer cells to promote pulmonary metastasis. *J. Biol. Chem.* **283**, 7616-7627.
Huttenlocher, A., Lakonishok, M., Kinder, M., Wu, S., Truong, T., Knudsen, K. A. and Horwitz, A. F. (1998). Integrin and cadherin synergy regulates contact inhibition of migration and motile activity. *J. Cell Biol.* **141**, 515-526.
Janssens, K., Sung, H.-H. and Rørth, P. (2010). Direct detection of guidance receptor activity during border cell migration. *Proc. Natl. Acad. Sci. USA* **107**, 7323-7328.
Kühl, M. and Wedlich, D. (1996). Xenopus cadherins: sorting out types and functions in embryogenesis. *Dev. Dyn.* **207**, 121-134.
Lambert, O., Taveau, J.-C., Him, J. L. K., Al Kurdi, R., Gulino-Debrac, D. and Brisson, A. (2005). The basic framework of VE-cadherin junctions revealed by cryo-EM. *J. Mol. Biol.* **346**, 1193-1196.
Lee, H.-S., Mood, K., Battu, G., Ji, Y. J., Singh, A. and Daar, I. O. (2009). Fibroblast growth factor receptor-induced phosphorylation of ephrinB1 modulates its interaction with Dishevelled. *Mol. Biol. Cell.* **20**, 124-133.
Lewellyn, L., Cetera, M. and Horne-Badovinac, S. (2013). Misshapen decreases integrin levels to promote epithelial motility and planar polarity in Drosophila. *J. Cell Biol.* **200**, 721-729.
Lin, B., Yin, T., Wu, Y. I., Inoue, T. and Levchenko, A. (2015). Interplay between chemotaxis and contact inhibition of locomotion determines exploratory cell migration. *Nat. Commun.* **6**, 6619.
Luu, O., Nagel, M., Wacker, S., Lemaire, P. and Winklbauer, R. (2008). Control of gastrula cell motility by the Goosecoid/Mix.1/Siamois network: basic patterns and paradoxical effects. *Dev. Dyn.* **237**, 1307-1320.
Matthews, H. K., Marchant, L., Carmona-Fontaine, C., Kuriyama, S., Larraín, J., Holt, M. R., Parsons, M. and Mayor, R. (2008). Directional migration of neural crest cells in vivo is regulated by Syndecan-4/Rac1 and non-canonical Wnt signaling/RhoA. *Development* **135**, 1771-1780.
McConnell, R. E., Edward van Veen, J., Vidaki, M., Kwiatkowski, A. V., Meyer, A. S. and Gertler, F. B. (2016). A requirement for filopodia extension toward Slit during Robo-mediated axon repulsion. *J. Cell Biol.* **213**, 261-274.
Mercola, M., Melton, D. A. and Stiles, C. D. (1988). Platelet-derived growth factor A chain is maternally encoded in Xenopus embryos. *Science* **241**, 1223-1225.
Mercola, M., Deininger, P. L., Shamah, S. M., Porter, J., Wang, C. Y. and Stiles, C. D. (1990). Dominant-negative mutants of a platelet-derived growth factor gene. *Genes Dev.* **4**, 2333-2341.
Morgan, M. R., Hamidi, H., Bass, M. D., Warwood, S., Ballestrem, C. and Humphries, M. J. (2013). Syndecan-4 phosphorylation is a control point for integrin recycling. *Dev. Cell* **24**, 472-485.
Morita, H., Kajiura-Kobayashi, H., Takagi, C., Yamamoto, T.S., Nonaka, S. and Ueno, N. (2012). Cell movements of the deep layer of non-neural ectoderm underlie complete neural tube closure in Xenopus. *Development* **139**, 1417-1426.
Muñoz, R., Moreno, M., Oliva, C., Orbenes, C. and Larraín, J. (2006). Syndecan-4 regulates non-canonical Wnt signalling and is essential for convergent and extension movements in Xenopus embryos. *Nat. Cell Biol.* **8**, 492-500.
Nagel, M. and Winklbauer, R. (1999). Establishment of substratum polarity in the blastocoel roof of the Xenopus embryo. *Development* **126**, 1975-1984.
Nagel, M., Tahinci, E., Symes, K. and Winklbauer, R. (2004). Guidance of mesoderm cell migration in the Xenopus gastrula requires PDGF signaling. *Development* **131**, 2727-2736.
Nagel, M., Luu, O., Bisson, N., Macanovic, B., Moss, T. and Winklbauer, R. (2009). Role of p21-activated kinase in cell polarity and directional mesendoderm migration in the Xenopus gastrula. *Dev. Dyn.* **238**, 1709-1726.
Nakatsuji, N., Smolira, M. A. and Wylie, C. C. (1985). Fibronectin visualized by scanning electron microscopy immunocytochemistry on the substratum for cell migration in Xenopus laevis gastrulae. *Dev. Biol.* **107**, 264-268.
Nieuwkoop, P. D. and Faber, J. (1967). *Normal Table of Xenopus laevis (Daudin)*. Amsterdam: North-Holland Publishing Company.
Niewiadomska, P., Godt, D. and Tepass, U. (1999). DE-Cadherin is required for intercellular motility during Drosophila oogenesis. *J. Cell Biol.* **144**, 533-547.
Ninomiya, H., David, R., Damm, E. W., Fagotto, F., Niessen, C. M. and Winklbauer, R. (2012). Cadherin-dependent differential cell adhesion in Xenopus causes cell sorting in vitro but not in the embryo. *J. Cell Sci.* **125**, 1877-1883.
Ohkawara, B., Glinka, A. and Niehrs, C. (2011). Rspo3 binds syndecan 4 and induces Wnt/PCP signaling via clathrin-mediated endocytosis to promote morphogenesis. *Dev. Cell* **20**, 303-314.
Poitras, L., Jean, S., Islam, N. and Moss, T. (2003). PAK interacts with NCK and MLK2 to regulate the activation of jun N-terminal kinase. *FEBS Lett.* **543**, 129-135.
Ramos, J. W. and DeSimone, D. W. (1996). Xenopus embryonic cell adhesion to fibronectin: position-specific activation of RGD/synergy site-dependent migratory behavior at gastrulation. *J. Cell Biol.* **134**, 227-240.
Rohani, N., Canty, L., Luu, O., Fagotto, F. and Winklbauer, R. (2011). EphrinB/EphB signaling controls embryonic germ layer separation by contact-induced cell detachment. *PLoS Biol.* **9**, e1000597.
Rohani, N., Parmeggiani, A., Winklbauer, R. and Fagotto, F. (2014). Variable combinations of specific ephrin ligand/Eph receptor pairs control embryonic tissue separation. *PLoS Biol.* **12**, e1001955.
Roper, J. A., Williamson, R. C. and Bass, M. D. (2012). Syndecan and integrin interactomes: large complexes in small spaces. *Curr. Opin. Struct. Biol.* **22**, 583-590.
Scarpa, E., Szabó, A., Bibonne, A., Theveneau, E., Parsons, M. and Mayor, R. (2015). Cadherin switch during EMT in neural crest cells leads to contact inhibition of locomotion via repolarization of forces. *Dev. Cell* **34**, 421-434.
Schwarzbauer, J. E. and DeSimone, D. W. (2011). Fibronectins, their fibrillogenesis, and in vivo functions. *Cold Spring Harb. Perspect. Biol.* **3**, a005041.
Smith, E. M., Mitsi, M., Nugent, M. A. and Symes, K. (2009). PDGF-A interactions with fibronectin reveal a critical role for heparan sulfate in directed cell migration during Xenopus gastrulation. *Proc. Natl. Acad. Sci. USA* **106**, 21683-21688.
Stramer, B. and Mayor, R. (2016). Mechanisms and in vivo functions of contact inhibition of locomotion. *Nat. Rev. Mol. Cell Biol.* **18**, 43-55.
Tanaka, M., Kuriyama, S. and Aiba, N. (2012). Nm23-H1 regulates contact inhibition of locomotion, which is affected by ephrin-B1. *J. Cell Sci.* **125**, 4343-4353.
Tanaka, R., Seki, Y., Saito, Y., Kamiya, S., Fujita, M., Okutsu, H., Iyoda, T., Takai, T., Owaki, T., Yajima, H. et al. (2014). Tenascin-C-derived peptide TNIIIA2 highly enhances cell survival and platelet-derived growth factor (PDGF)-dependent cell proliferation through potentiated and sustained activation of integrin α5β1. *J. Biol. Chem.* **289**, 17699-17708.
Vasilyev, A., Liu, Y., Mudumana, S., Mangos, S., Lam, P.-Y., Majumdar, A., Zhao, J., Poon, K.-L., Kondrychyn, I., Korzh, V. et al. (2009). Collective cell migration drives morphogenesis of the kidney nephron. *PLoS Biol.* **7**, e9.
Veevers-Lowe, J., Ball, S. G., Shuttleworth, A. and Kielty, C. M. (2011). Mesenchymal stem cell migration is regulated by fibronectin through α5β1-integrin-mediated activation of PDGFR-β and potentiation of growth factor signals. *J. Cell Sci.* **124**, 1288-1300.
Villar-Cerviño, V., Molano-Mazón, M., Catchpole, T., Valdeolmillos, M., Henkemeyer, M., Martínez, L. M., Borrell, V. and Marín, O. (2013). Contact repulsion controls the dispersion and final distribution of Cajal-Retzius cells. *Neuron* **77**, 457-471.
Wacker, S., Brodbeck, A., Lemaire, P., Niehrs, C. and Winklbauer, R. (1998). Patterns and control of cell motility in the Xenopus gastrula. *Development* **125**, 1931-1942.
Wen, J. W. H. and Winklbauer, R. (2017). Ingression-type cell migration drives vegetal endoderm internalisation in the Xenopus gastrula. *eLife* **6**, e27190.
Whittaker, C. A. and DeSimone, D. W. (1993). Integrin alpha subunit mRNAs are differentially expressed in early Xenopus embryos. *Development* **117**, 1239-1249.
Winklbauer, R. (1990). Mesodermal cell migration during Xenopus gastrulation. *Dev. Biol.* **142**, 155-168.
Winklbauer, R. (1998). Conditions for fibronectin fibril formation in the early Xenopus embryo. *Dev. Dyn.* **212**, 335-345.
Winklbauer, R. (2009). Cell adhesion in amphibian gastrulation. *Internatl. Review Cell. Mol. Biol.* **278**, 215-275.
Winklbauer, R. and Keller, R. E. (1996). Fibronectin, mesoderm migration, and gastrulation in Xenopus. *Dev. Biol.* **177**, 413-426.
Winklbauer, R. and Nagel, M. (1991). Directional mesoderm cell migration in the Xenopus gastrula. *Dev. Biol.* **148**, 573-589.
Winklbauer, R. and Schürfeld, M. (1999). Vegetal rotation, a new gastrulation movement involved in the internalization of the mesoderm and endoderm in Xenopus. *Development* **126**, 3703-3713.
Winklbauer, R. and Selchow, A. (1992). Motile behavior and protrusive activity of migratory mesoderm cells from the Xenopus gastrula. *Dev. Biol.* **150**, 335-351.
Winklbauer, R. and Stoltz, C. (1995). Fibronectin fibril growth in the extracellular matrix of the Xenopus embryo. *J. Cell Sci.* **108**, 1575-1586.
Winklbauer, R., Selchow, A., Nagel, M. and Angres, B. (1992). Cell interaction and its role in mesoderm cell migration during Xenopus gastrulation. *Dev. Dyn.* **195**, 290-302.
Xu, K., Tzvetkova-Robev, D., Xu, Y., Goldgur, Y., Chan, Y.-P., Himanen, J. P. and Nicolov, D. B. (2013). Insights into Eph receptor tyrosine kinase activation from crystal structures of the EphA4 ectodomain and its complex with ephrin-A5. *Proc. Natl. Acad. Sci. USA* **110**, 14634-14639.
Zantek, N. D., Azimi, M., Fedor-Chaiken, M., Wang, B., Brackenbury, R. and Kinch, M. S. (1999). E-cadherin regulates the function of the EphA2 receptor tyrosine kinase. *Cell Growth Differ.* **10**, 629-638.
Zhang, Z., Rankin, S. A. and Zorn, A. M. (2016). Syndecan4 coordinates Wnt/JNK and BMP signaling to regulate foregut progenitor development. *Dev. Biol.* **416**, 187-199.

Table S1. mRNA amounts injected per blastomere

mRNA amounts injected per blastomere:	
KD-PDGFR	100pg
mbGFP	150pg
mbRFP	100pg
KD-Pak1	300pg
CA-Pak1	40pg
eB1-mCherry	200pg
lf-PDGF-A	400pg
mPDGFdn	200pg

Table S2. Morpholino antisense oligonucleotides

Target	Sequence	Injection per blastomere
ephrinB1[1]	5' GGAGCCCTTCCATCCGCACAGGTGG 3'	20ng
ephrinB2[1]	5' ACACCGAGTCCCCGCTCAGTGCCAT 3'	20ng
xFN1[2]	5' CGCTCTGGAGACTATAAAAGCCAAT 3'	18ng
xFN2[2]	5' CGCATTTTTCAAACGCTCTGAAGAC 3'	18ng
xSyn4.1[3]	5' GCACAAACAGCAGGGTCGGACTCAT 3'	18ng
xSyn4.2[3]	5' CTAAAAGCAGCAGGAGGCGATTCAT 3'	18ng
xIntβ1[4]	5' GTGAATACTGGATAATGGGCCATCT 3'	20ng
xC-cadh.[5]	5' CCACCGTCCCGAACAGAAGCCTCAT 3'	20ng

All morpholinos have been characterized previously: [1]Rohani et al. (2011, 2014); Wen and Winklbauer (2017); [2]Davidson et al. (2006); [3]Munoz et al. (2006); Matthews et al. (2008); Ohkawara et al. (2011); Zhang et al. (2016); [4]Morita et al. 2012; [5]Ninomiya et al. (2012).

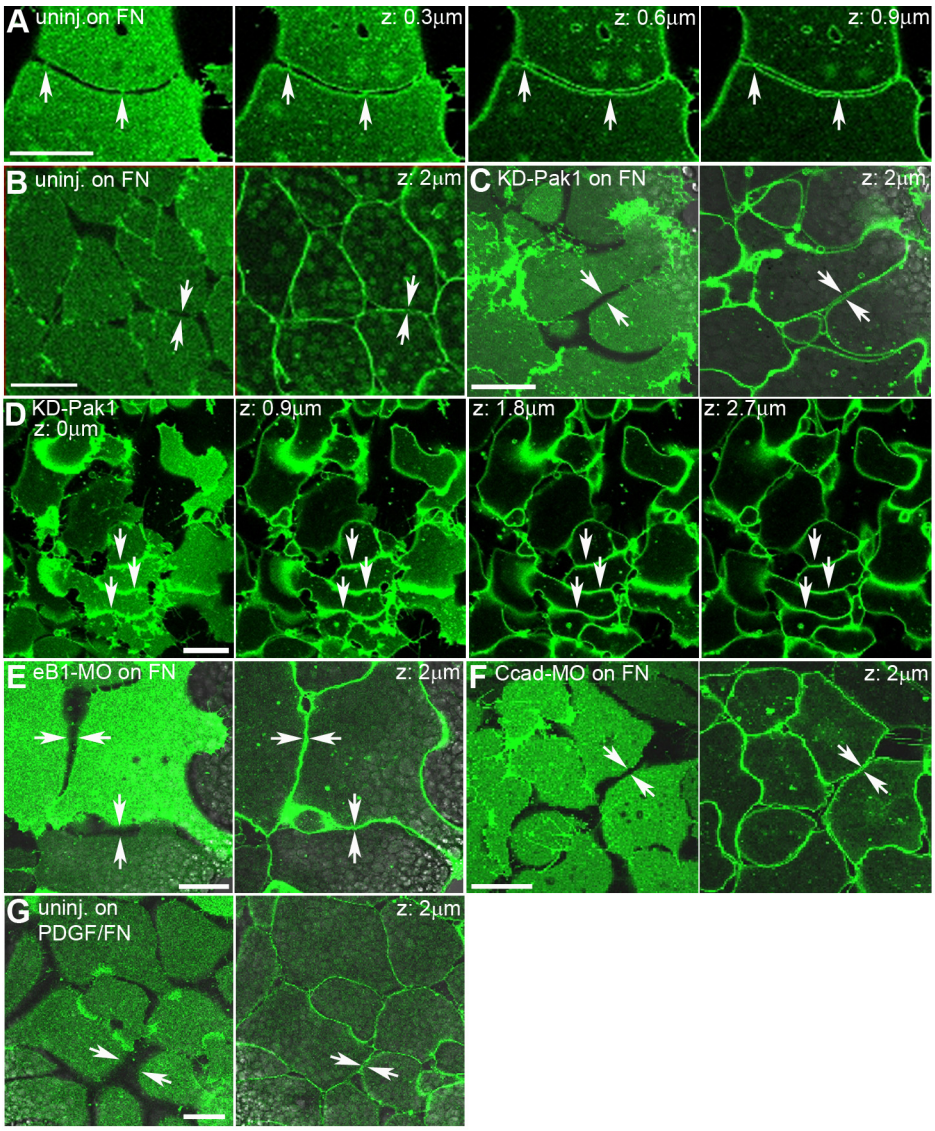

Figure S1. Cell contacts in aggregates. (A) Z-stack of an apposed cell pair on FN. Tiny processes (white arrows) bridge narrow gaps between cells at different levels above the substratum. (B) In aggregates cells are separated by small gaps (white arrow pairs) where attached to the FN substratum, but are more tightly packed above the substratum level. (C,D) In KD-Pak1 expressing aggregates cells are less densely packed at the FN substratum, with irregular gaps between cells, but tightly packed above. Underlapping cells are closely attached interiorly (D). (E–G) Cells are loosely packed in ephrinB1-MO aggregates (E) and C-cad-MO aggregates (F) on FN and in untreated aggregates on PDGF/FN substratum (G). Bars are 30 µm.

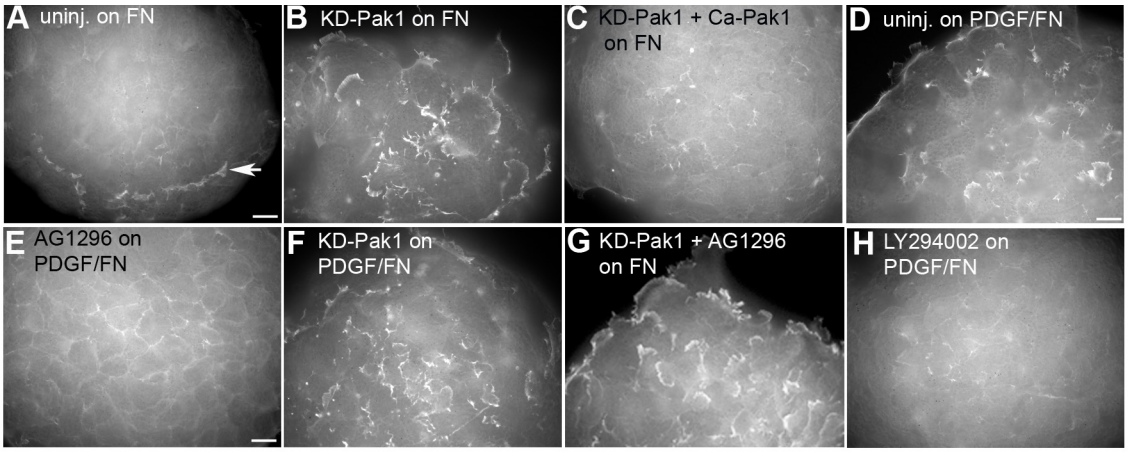

Figure S2. Lamelliform protrusions in fixed aggregates visualized by phalloidin-fluorescein staining of F-actin. In untreated aggregates on FN (A) Cells only show lamellipodia at the margin (white arrow). Sub-marginal lamellipodia were induced by KD-Pak1 (B), and the effect was reversed by co-expression of constitutively active CA-Pak1(C). Aggregates on PDGF-FN (D) show submarginal protrusions which were suppressed by the PDGFR inhibitor AG1296 (E) and the PI3K inhibitor LY294002 (H). DN-Pak1 augments lamellipodia formation on PDGF-FN (F) and rescues submarginal lamellipodia suppressed by AG 1296 (G). Bars are 30 μm.

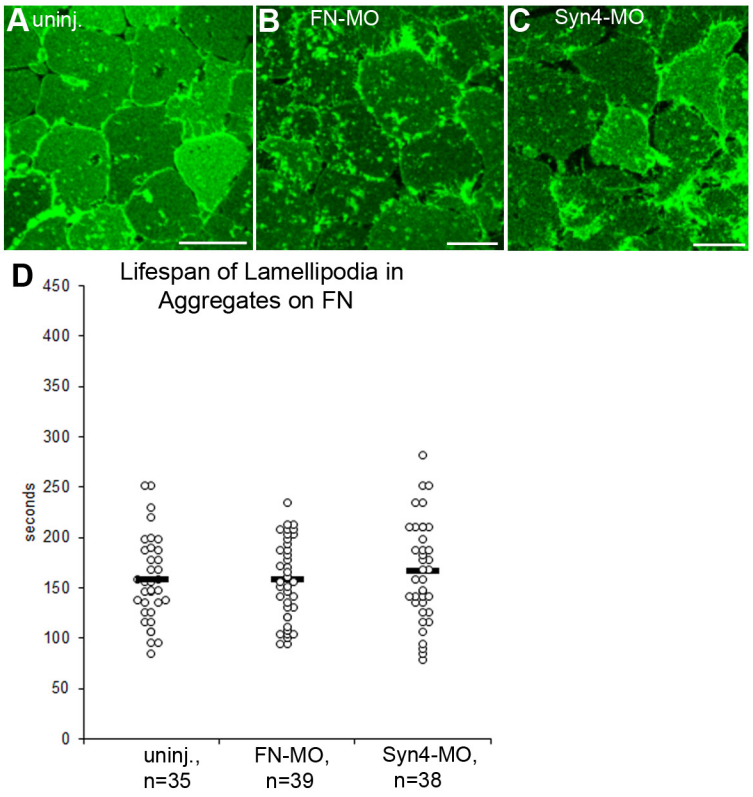

Figure S3. Knockdown of csFN or syndecan-4 has no effect on submarginal lamellipodia. (A) uninjected, (B) FN-MO injected and (C) Syn-4-MO injected explants on FN substratum, labeled with membrane-GFP. (D) Lifespan of lamellipodia.

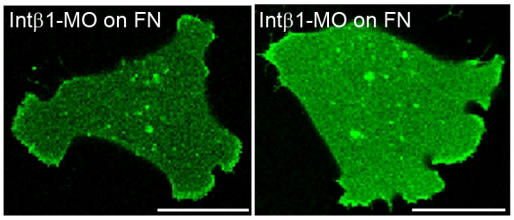

Figure S4. Single cells injected with integrin-MO on FN substratum. Bars are 30 μm.

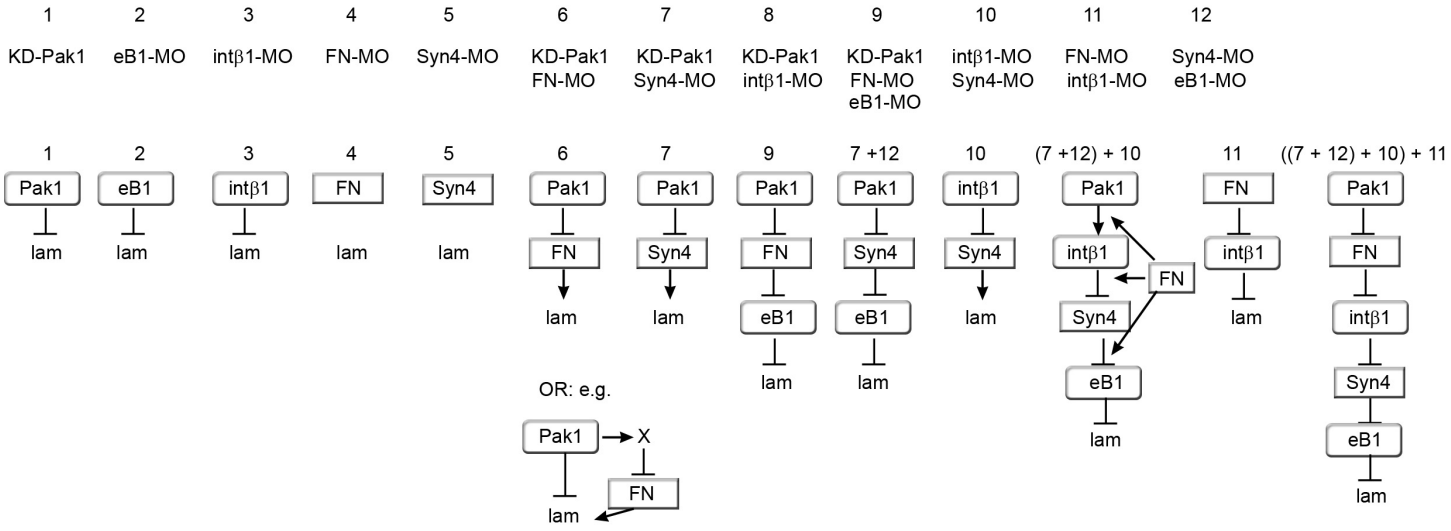

Figure S5. Step-by-step construction of the epistatic interaction module for contact inhibition of lamellipodia. Top row, relevant experimental treatments of LEM explants on FN substratum, numbered for identification. Below, epistatic relationships deduced from respective treatments. Inhibition of Pak1, ephrinB1 (eB1) and integrin β1 (intβ1) relieve contact inhibition, indicating that these factors promote lamellipodia collapse (inhibitory arrows) when active (round cartouches) (1-3). Inhibition of fibronectin (FN) and syndecan-4 (syn4) alone have no effect, suggesting that they are not active (rectangular cartouches) in normal explants (4,5). Inhibition of these factors reverses the effects of Pak1 inhibition, placing them downstream of Pak1 (6,7). Alternatively, they could act in parallel pathways, but since they interact with Pak1, this would require additional factors (e.g. X) and additional interactions (e.g. 6, bottom). In the absence of any evidence for such additional components, we always assume in the following the simplest possible interactions. eB1 reverses the effects of FN or syn4 downstream of Pak1, placing it downstream of these factors (9, 7+12), and syn4 inhibition reverses the effect of intβ1 inhibition, placing it downstream (10). Combining (7+12) and (10) orders Pak1, intβ1, syn4, and eB1, and since (11) indicates that intβ1 acts downstream of FN, the final sequence of components is derived (last column). That all interactions are inhibitory is contingent in the sense that the list of participating components is not necessarily complete. With additional components, further inhibitory, or activating interactions could become introduced.

Movies

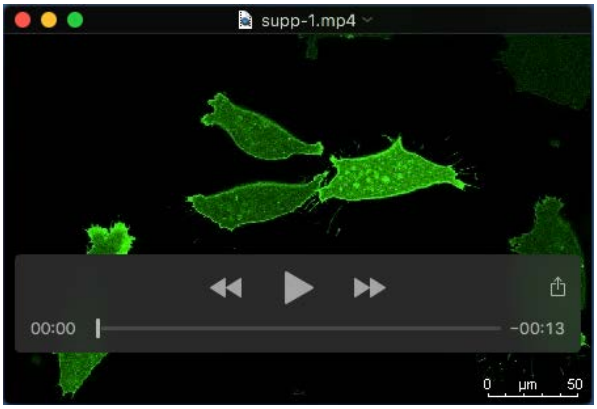

Movie 1. Protrusion formation and behavior of single mesoderm cells on FN. The confocal time lapse recording shows dissociated mesoderm cells expressing mb-GFP migrating on a FN coated dish. Cells extend lamelliform protrusions, which collapse immediately after contact with another cell.

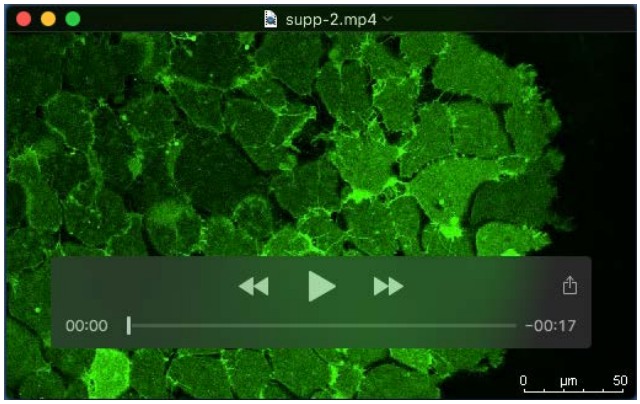

Movie 2. Protrusive activity in mesoderm aggregates on FN. In this confocal time lapse recording of an mb-GFP expressing mesoderm aggregate on FN substratum, small short-lived protrusions form which collapse immediately after contact with adjacent cells. On the free margin (right side) cells extend long-lived lamellipodia.

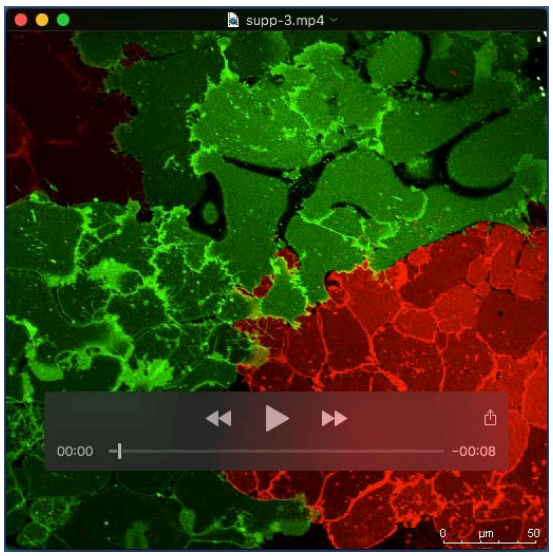

Movie 3. In kinase-dead Pak1 expressing aggregates cells overcome contact inhibition of lamellipodia. A time lapse recording of a KD-Pak1 expressing aggregate (green, mb-GFP) is shown side by side with an untreated aggregate (red, mb-RFP) on a FN coated dish. The KD-Pak1 expressing cells show an increased number of large protrusions with an increased survival time. Untreated cells in the aggregate are more densely packed and have only small short lived protrusions.

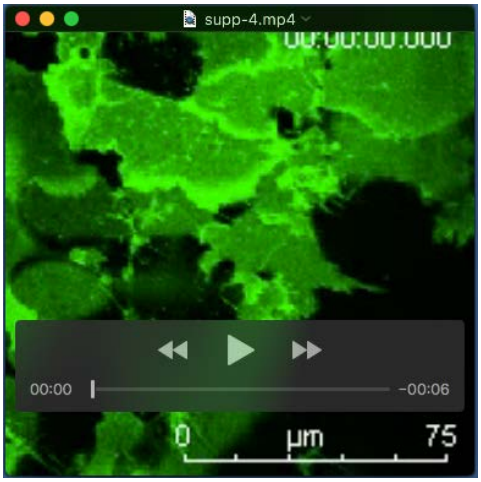

Movie 4. Expression of kinase-dead Pak1 in aggregates leads to the formation of chains of underlapping cells. The time lapse recording shows cells underlapping each other, with the lamellipodia pointing in the same direction.

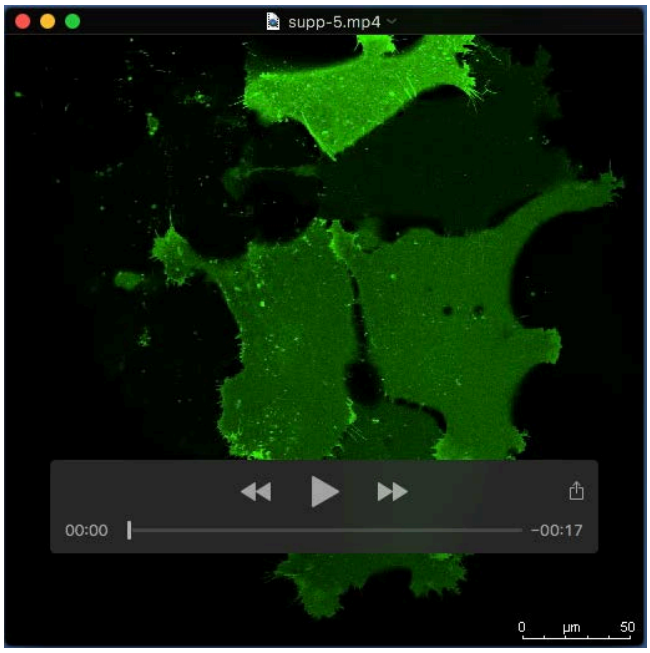

Movie 5. Knockdown of ephrinB1 stimulates sub-marginal protrusion formation. Time lapse recording shows an aggregate injected with ephrinB1-MO. Cells underlap each other with large smooth-rimmed lamellipodia.

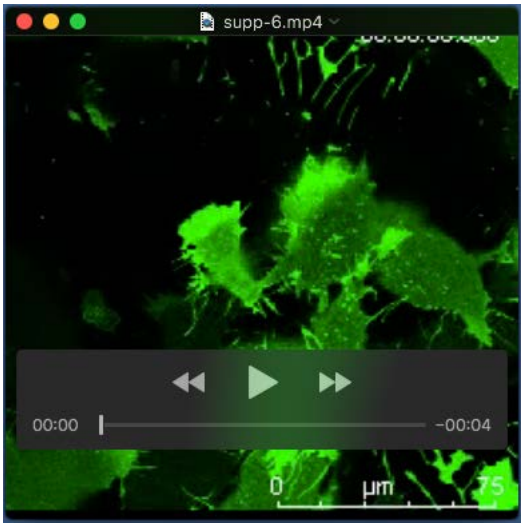

Movie 6. Knockdown of ephrinB1 leads to formation of shingle arrangement. The time lapse recording shows cells underlapping each other in series, with the lamellipodia pointing in the same direction.

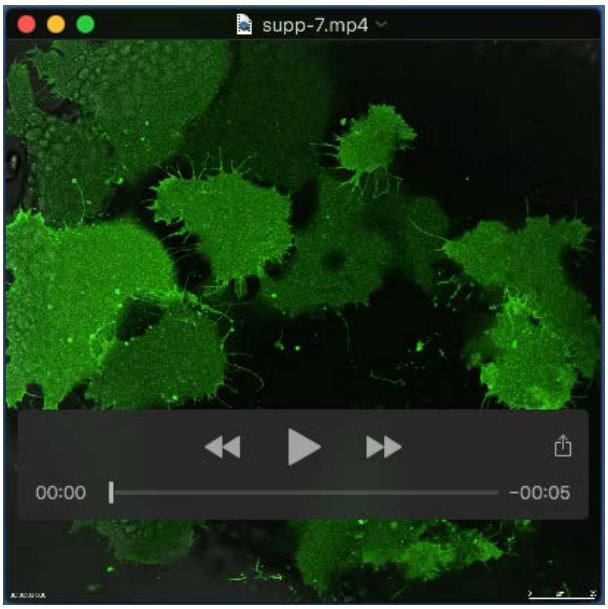

Movie 7. Injection of FN-MO together with KD-Pak1 mRNA leads to rapid collapse of lamellipodia. In this time lapse recording cells in the aggregate form large lamellipodia which rapidly switch to filopodia extension, and retreat, leaving retraction fibers behind.

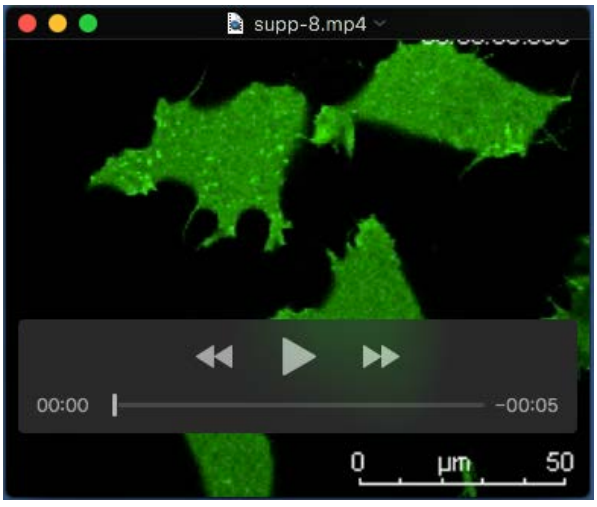

Movie 8. Protrusion formation and behavior of single mesoderm cells on FN-PDGF. In the time lapse recording single cells are seen to migrate on an FN-PDGF coated dish. They form large lamellipodia and often underlap each other when they meet..

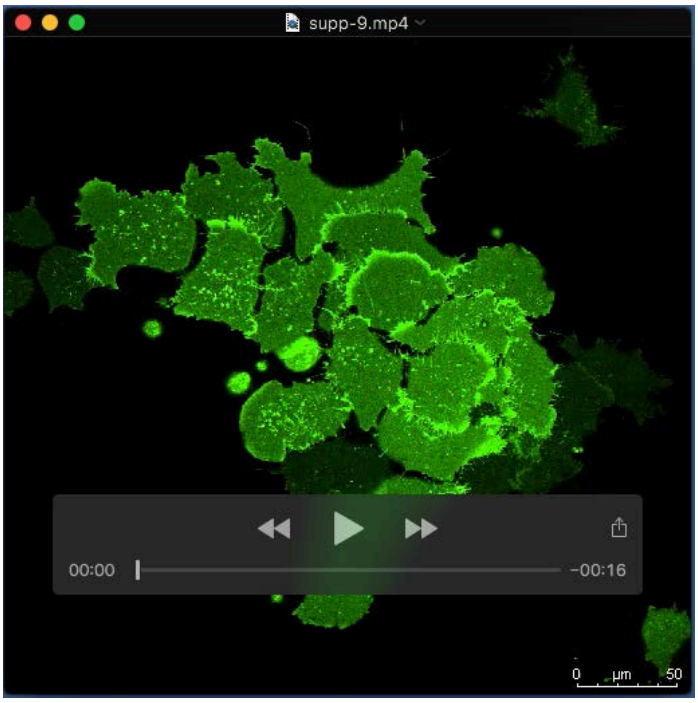

Movie 9. PDGF signaling promotes sub-marginal protrusion formation in LEM aggregates. The time lapse recording shows mesoderm aggregate on FN-PDGF substratum, where cells underlap each other with large, smooth lamellipodia and can form shingle arrangements.